ORGANOMETALLICS

Article

pubs.acs.org/Organometallics

Highly Electron-Rich Pincer-Type Iron Complexes Bearing Innocent Bis(metallylene)pyridine Ligands: Syntheses, Structures, and Catalytic Activity

Daniel Gallego, Shigeyoshi Inoue, Burgert Blom, and Matthias Driess*

Department of Chemistry: Metalorganics and Inorganic Materials, Technische Universität Berlin, Straße des 17. Juni 135, Sekr. C2, 10623 Berlin, Germany

Supporting Information

ABSTRACT: The first neutral bis(metallylene)pyridine pincer-type [**ENE**] ligands (E = Si^{II}, Ge^{II}) were synthesized, and their coordination chemistry and reactivity toward iron was studied. First, the unprecedented four-coordinate complexes κ^2***E,E′***-[**ENE**]**FeCl$_2$** were isolated. Unexpectedly and in contrast to other related pyridine-based pincer-type Fe(II) complexes, the N atom of pyridine is reluctant to coordinate to the Fe(II) site due to the enhanced σ-donor strength of the E atoms, which disfavors this coordination mode. Subsequent reduction of κ^2***Si,Si′***-[**SiNSi**]**FeCl$_2$** with KC_8 in the presence of PMe_3 or direct reaction of the [**ENE**] ligands using $Fe(PMe_3)_4$ produced the highly electron-rich iron(0) complexes [**ENE**]-**Fe(PMe$_3$)$_2$**. The reduction of the iron center substantially changes its coordination features, as shown by the results of a single-crystal X-ray diffraction analysis of [**SiNSi**]**Fe(PMe$_3$)$_2$**. The iron center, in the latter, exhibits a pseudosquare pyramidal (PSQP) coordination environment, with a coordinative (pyridine)N→Fe bond, and a trimethylphosphine ligand occupying the apical position. This geometry is very unusual for Fe(0) low-spin complexes, and variable-temperature ^{1}H and ^{31}P NMR spectra of the [**ENE**]**Fe(PMe$_3$)$_2$** complexes revealed that they represent the first examples of configurationally stable PSQP-coordinated Fe(0) complexes: even after heating at 70 °C for >7 days, no changes are observed. The substitution reaction of [**ENE**]**Fe(PMe$_3$)$_2$** with CO resulted in the isolation of [**ENE**]**Fe(CO)$_2$** and the hitherto unknown κ^2***E,E′***-[**ENE**]**Fe(CO)$_2$L** (L = CO, PMe_3) complexes. All complexes were fully characterized (NMR, MS, XRD, IR, and ^{57}Fe Mössbauer spectroscopy), showing the highest electron density on the iron center for pincer-type complexes reported to date. DFT calculations and ^{57}Fe Mössbauer spectroscopy confirmed the innocent behavior of these ligands. Moreover, preliminary results showed that these complexes can serve as active precatalysts for the hydrosilylation of ketones.

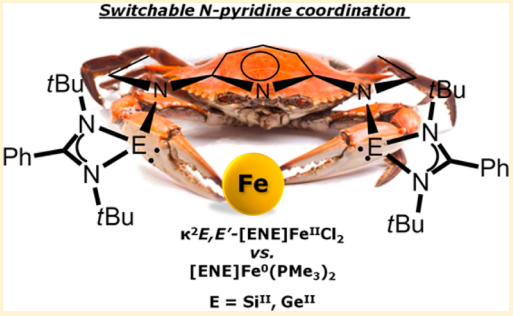

INTRODUCTION

Ligand design plays a crucial role in tuning the reactivity of transition metal (TM) centers in organometallic chemistry.[1] Multidentate donor ligands have the advantage that they can simultaneously increase the electronic density and stabilize the coordination sphere of a TM. In particular, the pincer-type motif [EDE], featuring a tridentate, meridional coordinating ligand framework, offers a myriad of opportunities for controlling the steric and electronic properties of TM complexes.[2] Generally, the side arms of a pincer ligand consist of neutral, two-electron Lewis donor moieties (e.g., E = PR_2, NR_2, or SR), which are connected through a linker group (often CH_2 or O) to a neutral or monoanionic anchoring site D (e.g., pyridyl or phenyl group). During the past decade, several groups have employed such ligands for stabilizing low-valent first-row TM complexes, particularly iron(0) complexes (Figure 1). As a seminal example, employing a bis(imino)pyridine of type [NNN], Chirik and co-workers[3] stabilized a bis-(dinitrogen)iron complex **I**; however the correct description of the electronic ground state is a biradical [$NNN^{2\bullet-}$]Fe(II)-$(N_2)_2$ rather than Fe(0), due to the noninnocence of the bis(imino)pyridine ligand.[4,5] Other research groups have applied different pincer-type systems to stabilize other low-valent iron complexes. Danopoulos and co-workers reported a bis(carbene)pyridine ligand stabilizing the bis(dinitrogen)iron [CNC]$Fe(N_2)_2$ complex **II**.[6] It has also been shown that pincer-stabilized iron(0) complexes are the active species in catalytic reactions such as alkene hydrosilylation and asymmetric hydrogenation of ketones and imines by isolating their bis-carbonyl complexes.[7,8] Recently, Milstein and co-workers demonstrated the noninnocent behavior of bipyridine-based PNN pincer ligands with iron biscarbonyl complexes **III**.[9] In addition to these seminal efforts, other ligand systems have been applied for the stabilization of reactive iron(0) complexes. Fürstner and co-workers[10] demonstrated the remarkable ability of iron(0)-ate complexes **IV** to serve as active catalysts in the cycloisomerization of enynes. More recently, the research groups of Peters[11] and Deng[12] also reported fascinating

Received: September 22, 2014
Published: November 23, 2014

   dx.doi.org/10.1021/om500966t | *Organometallics* 2014, 33, 6885−6897

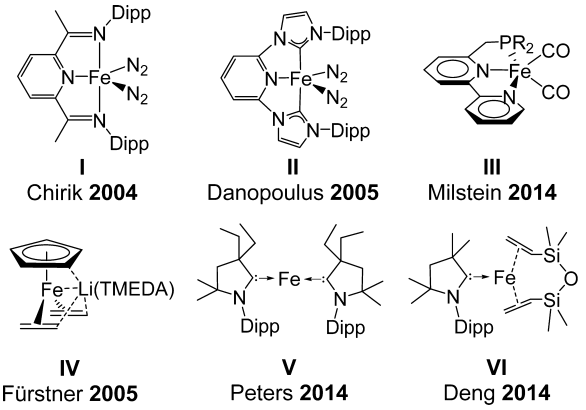

Figure 1. Examples of isolable iron(0) complexes for activation of strong σ-bonds and/or catalytic applications.

examples for the stabilization of highly reactive low-coordinate iron(0) compounds (**V** and **VI**, Figure 1).

In addition to their interesting structural features, iron-based pincer-type complexes present high catalytic activity for different reactions such as hydrogenation,[8,13,14] hydrosilylation,[3,15] and hydroboration.[16] Recently, we reported the first example of a highly electron-rich iron(0) complex stabilized by a hydrido-silylene ligand (Scheme 1).[17] This complex was found to be catalytically active toward hydrosilylation of ketones and demonstrated cooperativity between the metal center and the hydrido-silylene ligand. We have also recently investigated the potential application of bis(metallylene) pincer ligands in catalytic transformations such as borylation of arenes mediated by the [ECE]Ir complexes[18] and Sonogashira cross-coupling reactions effected by [ECE]Ni complexes[19] with E = Si^{II}, Ge^{II}. The latter studies revealed higher σ-donor strength compared with traditional P^{III}-based pincer ligands. These studies showed that metallylenes not only dramatically enhance the electron donor properties but play a crucial role in the catalytic behavior of their metal complexes. Inspired by these results, we envisaged the synthesis of a neutral bis(metallylene)-pyridine pincer-type ligand to study its coordination toward iron as a nontoxic, inexpensive, and abundant TM, with the aim to increase the electron density on iron(0) stabilized by a tridentate ligand for further catalytic application (Scheme 1).

Herein, we reported the synthesis of the first neutral bis(metallylene)pyridine pincer ligands of type **ENE** (E = Si^{II}, Ge^{II}) and their unexpected coordination mode toward iron as a nonprecious metal center in the different oxidation states 0 and +2. These studies revealed a novel coordination mode of Fe(II) in the $FeCl_2$ pincer complexes κ^2E,E'-[**ENE**]$FeCl_2$. In addition, we observed a strikingly high stability in solution for the novel iron(0) complexes of type [**ENE**]$Fe(PMe_3)_2$ without any observable Berry pseudorotation within a wide range of temperatures. These complexes represent a new family of highly electron-rich iron(0) complexes that can moreover act as precatalysts in the hydrosilylation of ketones.

RESULTS AND DISCUSSION

Synthesis of the ENE (E = Si^{II}, Ge^{II}) Pincer-Type Ligands. Continuing our studies on the low-valent group 14 pincer ligands of the type [ECXE] (E = Si^{II}, Ge^{II}; X = H, Br) as monoanionic tridentate chelate ligands toward TM centers of group 9 and 10, we envisaged the synthesis of neutral tridentate ligands based on bis(silylenes) and bis(germylenes) as σ-donors with a view to expand their chemistry toward the group 8 TMs. On the basis of our synthetic approach for the synthesis of these ligands, we planned the synthesis of the pyridine-based pincer ligands through salt metathesis reactions of 2,6-diamine-*N,N'*-diethylpyridine as the backbone. The synthesis of this disubstituted pyridine was carried out following the reported procedures for alkylation of amines.[20−22] Acetylation of the 2,6-diaminopyridine with concomitant reduction with lithium aluminum hydride (LAH) produced the desired 2,6-diamino-

Scheme 1. Earlier Work on Iron-Based Silylene Complex and Nickel-Based Bis(metallylene) Pincer Complexes in Catalysis and the Novel Iron-Based Bis(metallylene) Pincer Complexes

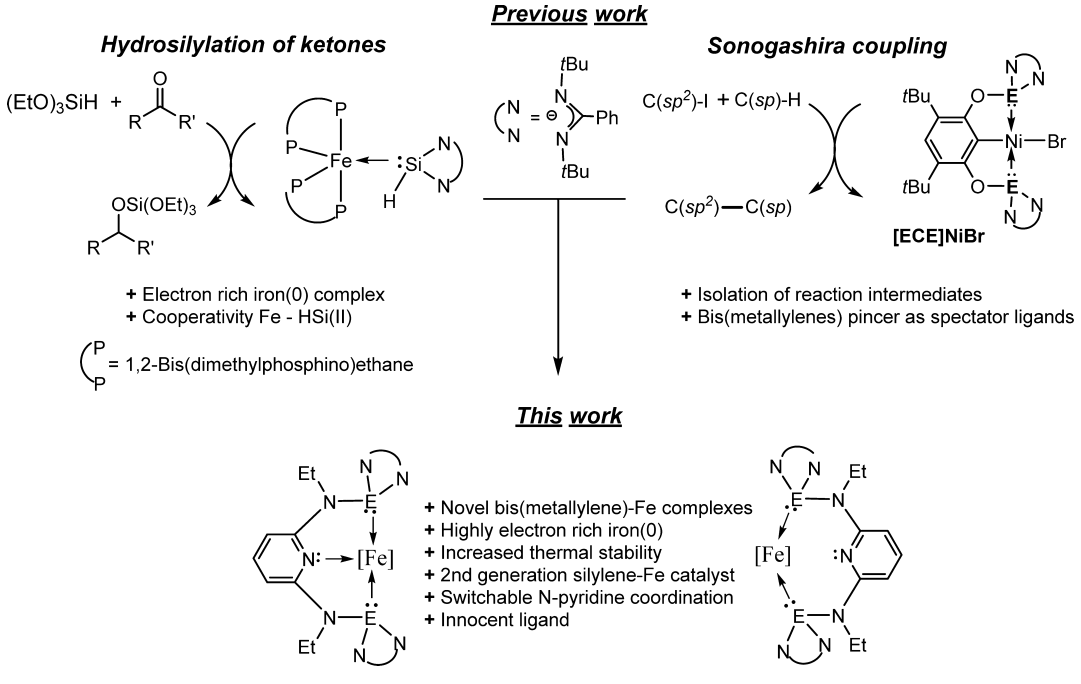

dx.doi.org/10.1021/om500966t | *Organometallics* 2014, 33, 6885−6897

N,N′-diethylpyridine. Deprotonation of the latter with 2 molar equiv of *n*-BuLi in refluxing diethyl ether, followed by the dropwise addition of 2 molar equiv of the *N,N′*-di-*tert*-butyl(phenylamidinato)chlorosilylene or -germylene in a toluene solution at −78 °C, afforded the desired **SiNSi** and **GeNGe** products after warming to room temperature overnight (Figure 2).

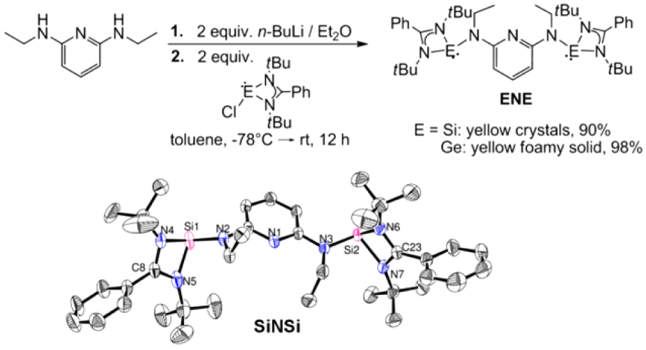

Figure 2. Synthesis of the neutral pincer ligands **ENE** (E = Si^{II}, Ge^{II}) and the ORTEP representation of the **SiNSi** ligand in the solid state. Thermal ellipsoids are drawn at the 50% probability level. Hydrogen and solvent atoms are omitted for clarity. Selected distances [Å] and angles [deg]: Si(1)−N(2) 1.7688(18), Si(1)−N(4) 1.8762(19), Si(2)−N(3) 1.7894(19), Si(2)−N(6) 1.8767(19), N(1)−C(1) 1.343(3), N(1)−C(5) 1.347(3), N(2)−C(1) 1.407(3), N(3)−C(5) 1.401(3), N(4)−Si(1)−N(5) 68.83(9), N(6)−Si(2)−N(7) 68.83(8), N(2)−Si(1)−N(4) 101.77(9), C(1)−N(2)−Si(1) 119.10(15), C(5)−N(3)−Si(2) 120.19(15). See Supporting Information for details.

The ^{1}H NMR spectra for **SiNSi** and **GeNGe** reveal a singlet resonance signal for the *tert*-butyl, a triplet for the methyl, and a quartet for the methylene moieties with the relative intensity of 18:3:2, respectively. Purification by extraction with *n*-hexane and recrystallization leads to analytically pure **SiNSi**. Somewhat noteworthy is that the **GeNGe** ligand exhibits a much higher solubility in organic solvents than its silicon analogue, which hampers crystallization. However, removal of the solvent *in vacuo* produced the desired ligand in high purity (>95%). Both ligands were fully characterized by ^{1}H, ^{13}C, and ^{29}Si NMR spectroscopy, high-resolution mass spectrometry, elemental analysis, and single-crystal X-ray diffraction analysis for **SiNSi** (see Experimental Section and Supporting Information). Interestingly, the NMR spectra of isolated crystals of **SiNSi** showed two sets of signals related to two rotational conformers in the pendant arms. For instance, the ^{29}Si NMR spectrum revealed three signals: one major signal at δ = −14.9 ppm and two other resonances at δ = −13.8 and −17.1 ppm, showing the inequivalency of the two silylene moieties. DOSY NMR studies permitted the unambiguous assignment of all signals to the same chemical species.

The single-crystal X-ray diffraction analysis for the **SiNSi** ligand reveals that only one of the conformers is present in the crystal lattice. The bond distances in the ligand backbone are almost unchanged after the new covalent bonds between the nitrogen and the silicon centers were formed. Both silylene subunits are pointing out of the pyridine moiety, but its fluxional behavior in solution, as confirmed by NMR, shows its possibility as a potential pincer-type ligand for a metal center in a meridional tridentate coordination.

Synthesis of the [ENE]$FeCl_2$ (E = Si^{II}, Ge^{II}) Complexes. The isolated **ENE** ligands were then employed as pincer ligands for iron. Reaction of the pincer ligands **ENE** (E = Si^{II}, Ge^{II}) with the *in situ* prepared $FeCl_2\cdot(thf)_{1.5}$ adduct afforded intense yellow solutions at room temperature (Scheme 2). Evaluation

Scheme 2. Synthesis of the κ^2E,E'-[ENE]$FeCl_2$ Complexes (E = Si^{II}, Ge^{II})

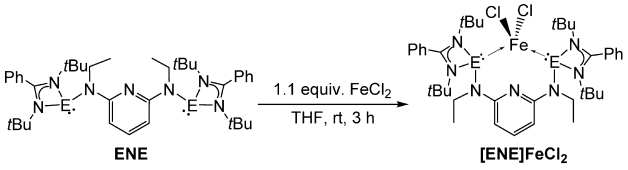

of the reaction mixtures by ^{1}H NMR showed paramagnetic spectra with broad signals at chemical shifts within the δ = −5 to +30 ppm range. Integration of the paramagnetically shifted signals however correlated with all the protons in the expected structure. Extraction and crystallization in toluene afforded yellow crystals in high yields (>70%). Their APCI HR-MS (atmospheric pressure chemical ionization high-resolution mass spectra) unambiguously proved the formation of the desired [**ENE**]$FeCl_2$ complexes ($M^{\bullet+}$, E = Si^{II}: calcd 807.30915; exptl 807.30914; E = Ge^{II}: calcd 899.19765; exptl 899.19928). Surprisingly, after growing suitable crystals for X-ray diffraction analysis we observed that the pyridine moiety most likely does not coordinate to the iron center, with N1−Fe interatomic distances of 3.304 and 3.543 Å for the bis(silylene) and bis(germylene) complexes, respectively. These distances are larger than the sum of covalent radii for nitrogen and iron, and the complexes are hence better described as κ^2E,E'-[**ENE**]-$FeCl_2$. This result contrasts with existing Fe(II) complexes with pyridine-based pincer ligands of type PNP, NNN, CNC, and NNP (Figure 3),[7,23a−e,24,25] in which a pentacoordinated iron center is present. This difference might be attributed to the enhanced σ-donor strength of the ENE ligands: first, the stronger σ-donor properties of the metallylenes[18,19] make the iron center more electron-rich, impeding 5-fold coordination, resulting in preferential tetrahedral coordination. Second, the high *trans* effect for the metallylenes might play a role in favoring the tetrahedral structure at the iron center.

The molecular structures depicted in Figure 4 show that the iron center exhibits a distorted tetrahedral coordination sphere in both complexes, being more similar to the literature examples where bidentate ligands such as bis-carbene (Figure 3)[24−26] or bis-phosphane[27] are employed. Both complexes crystallized in the monoclinic space group $P2_1/n$ having a C_{2v} symmetry where the vertical plane crosses the iron and chloride atoms. The Fe−Cl bond distances are within the range of the $FeCl_2$ complexes in a tetrahedral structure, but comparing the κ^2E,E'-[**ENE**]$FeCl_2$ (E = Si^{II}, Ge^{II}) complexes, there is an elongation in the bond distance of about 3.5−4.6 pm with the silylene as the σ-donor atom. Both structures are equivalent in their coordination sphere; therefore, this elongation is mainly due to the intrinsically higher σ-donor character of the silylene versus the germylene subunit. This increases the electronic density on the Fe(II) center, decreasing the interaction with the chloride ligands, which is in accord with our earlier observations.[18,19]

The electronic structures of the κ^2E,E'-[**ENE**]$FeCl_2$ complexes were in addition also studied by ^{57}Fe Mössbauer spectroscopy and solution magnetic moment studies (Evans

dx.doi.org/10.1021/om500966t | *Organometallics* 2014, 33, 6885−6897

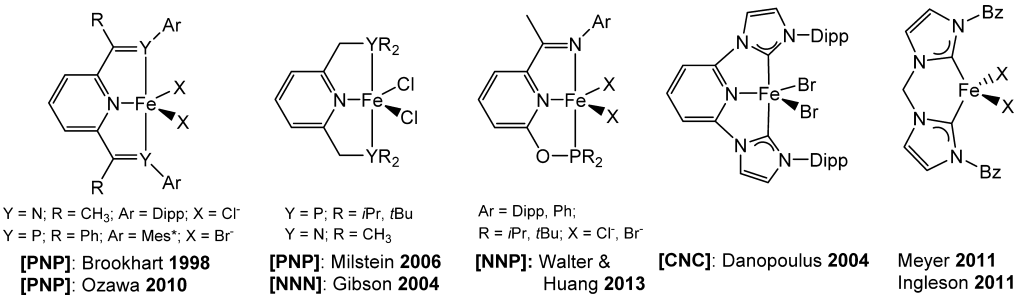

Figure 3. Some examples of Fe(II) complexes bearing pincer-type ligand moieties as well as a bis-N-heterocyclic carbene ligand for comparison.

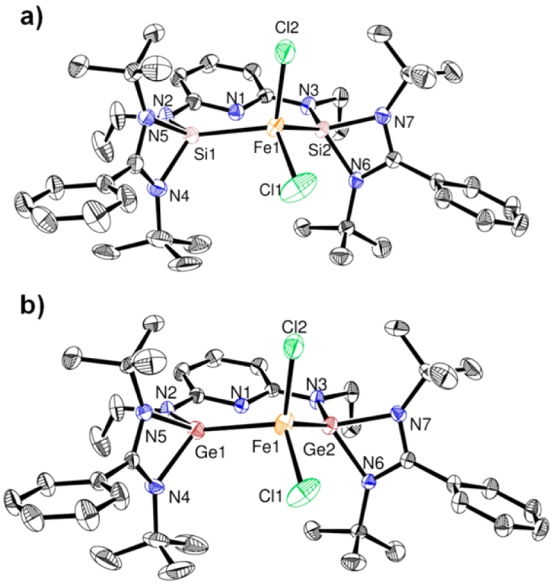

Figure 4. ORTEP representation of the κ^2E,E'-[ENE]$FeCl_2$ complexes in the solid state. Thermal ellipsoids are drawn at the 50% probability level. Hydrogen and solvent atoms are omitted for clarity. Selected distances [Å] and angles [deg]. (a) E = Si^{II}: Fe(1)−Si(1) 2.5256(7), Fe(1)−Si(2) 2.5110(7), Fe(1)−Cl(1) 2.2621(8), Fe(1)−Cl(2) 2.2819(8), Si(1)−N(2) 1.761(2), Si(1)−N(4) 1.855(2), Si(2)−N(3) 1.7608(19), Si(2)−Fe(1)−Si(1) 110.04(2), Cl(1)−Fe(1)−Cl(2) 113.23(4), Cl(1)−Fe(1)−Si(1) 110.09(4), Cl(2)−Fe(1)−Si(1) 107.39(3), Cl(1)−Fe(1)−Si(2) 108.82(3), Cl(2)−Fe(1)−Si(2) 107.22(3), N(2)−Si(1)−N(4) 104.93(10), N(4)−Si(1)−N(5) 70.22(9). (b) E = Ge^{II}: Fe(1)−Ge(1) 2.5670(4), Fe(1)−Ge(2) 2.5509(4), Fe(1)−Cl(1) 2.2268(7), Fe(1)−Cl(2) 2.2358(7), Ge(1)−N(2) 1.8739(18), Ge(1)−N(4) 1.9795(18), Ge(2)−N(3) 1.8661(16), Ge(2)−Fe(1)−Ge(1) 102.434(13), Cl(1)−Fe(1)−Cl(2) 120.17(3), Cl(1)−Fe(1)−Ge(1) 108.88(3), Cl(2)−Fe(1)−Ge(1) 107.34(2), Cl(1)−Fe(1)−Ge(2) 108.52(2), Cl(2)−Fe(1)−Ge(2) 108.06(2), N(2)−Ge(1)−N(4) 102.00(8), N(4)−Ge(1)−N(5) 65.95(7). See Supporting Information for details.

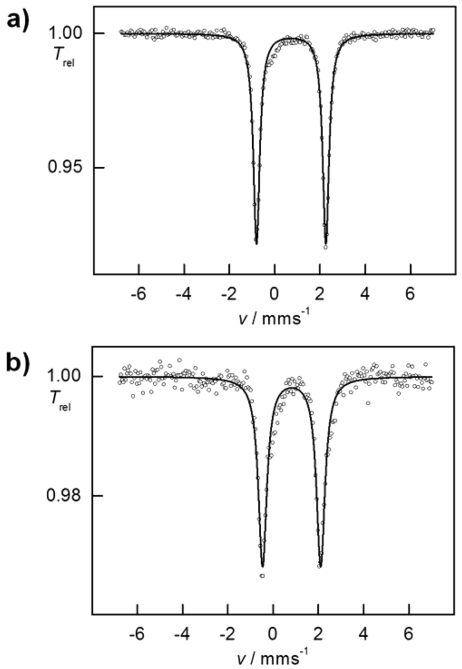

Figure 5. Zero-field ^{57}Fe Mössbauer spectra of complexes κ^2E,E'-[ENE]$FeCl_2$ at 77 K. The circles are experimental data, and the lines the simulated Lorentzian curves. (a) E = Si^{II}: δ = 0.73(1) mm s^{-1}, ΔE_Q = 3.06(1) mm s^{-1}, Γ_{fwhm} = 0.34(1) mm s^{-1}. (b) E = Ge^{II}: δ = 0.82(1) mm s^{-1}, ΔE_Q = 2.57(1) mm s^{-1}, Γ_{fwhm} = 0.46(1) mm s^{-1}.

method). From the ^{57}Fe Mössbauer spectra (Figure 5) the isomer shift (δ) and quadrupole splitting (ΔE_Q) values for these complexes are in accordance with the expectations for distorted tetrahedral high-spin Fe(II) complexes (δ = 0.73 mm s^{-1}, 0.82 mm s^{-1} and ΔE_Q = 3.06 mm s^{-1}, 2.57 mm s^{-1}, for E = Si^{II} and Ge^{II}).[24,25,27] This is, moreover, also in agreement with the experimentally determined magnetic moment in solution of μ_{eff} = 4.6 and 4.7 μB for E = Si^{II} and Ge^{II}, respectively, which also correspond to a high-spin S = 2 ground state.[24,28]

Synthesis of the [ENE]Fe(PMe$_3$)$_2$ (E = Si^{II}, Ge^{II}) Complexes. Low-valent iron complexes are extremely attractive for the activation of small molecules due to their high reactivity and potential application in catalytic systems. Due to the lack of coordination through the nitrogen on the pyridine backbone in the Fe(II) complexes, we envisaged that the reduction of the iron complexes under a nitrogen atmosphere could afford homologues of the bis(dinitrogen) iron pincer-like complexes (**I** and **II** in Figure 1) synthesized by Chirik[3] and Danopoulos.[6] Recently, we reported an arene iron(0) complex stabilized by a bis(carbene) ligand [Fe{(^{Dipp}C:)$_2$CH$_2$}(η^6-C_7H_8)] ((^{Dipp}C:)$_2$CH$_2$ = bis(*N*-Dipp-imidazole-2-ylidene)methylene),[26] and its comparison with its heavier homologues bis(silylene) and bis(germylene) would also be of interest, if isolable. Reduction of the Fe(II) complexes κ^2E,E'-[ENE]$FeCl_2$ with KC_8 in toluene/THF produced intense red solutions, although after workup and several unsuccessful attempts to crystallize a product we obtained a red oil as crude product. The ^{1}H NMR data suggest a ligand reduction is the major product along with other undefined side products but gave no hint for the formation of the envisaged arene or N_2 complex. This result prompted us to employ an alternative coligand that would possibly better stabilize the expected highly electron-rich iron(0) center after

dx.doi.org/10.1021/om500966t | *Organometallics* 2014, 33, 6885−6897

Scheme 3. Synthesis of the [ENE]Fe(PMe$_3$)$_2$ Pincer-like Complexes (E = Si^{II}, Ge^{II})

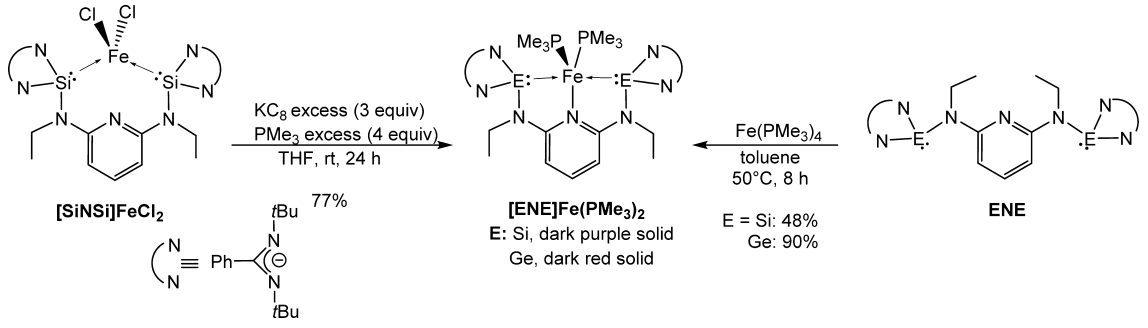

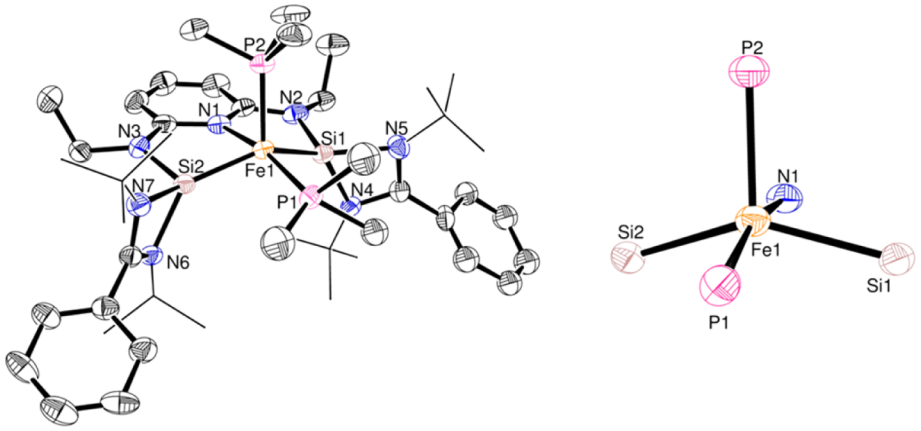

Figure 6. ORTEP representation of the [**SiNSi**]Fe(PMe$_3$)$_2$ complex in the solid state. Thermal ellipsoids are drawn at the 50% probability level. *tert*-Buyl groups are drawn with wireframe, and hydrogen atoms are omitted for clarity. Selected distances [Å] and angles [deg]: Fe(1)−N(1) 2.059(3), Fe(1)−Si(1) 2.1637(15), Fe(1)−Si(2) 2.1695(13), Fe(1)−P(1) 2.1455(11), Fe(1)−P(2) 2.1881(10), Si(1)−N(2) 1.790(4), Si(2)−N(3) 1.779(3), Si(1)−N(4) 1.927(4), N(1)−Fe(1)−P(1) 165.48(9), N(1)−Fe(1)−Si(1) 80.63(11), N(1)−Fe(1)−Si(2) 80.83(11), N(1)−Fe(1)−P(2) 86.80(9), P(1)−Fe(1)−Si(1) 94.19(5), P(1)−Fe(1)−Si(2) 95.38(5), P(1)−Fe(1)−P(2) 107.71(4), Si(1)−Fe(1)−P(2) 106.23(5), Si(2)−Fe(1)−P(2) 106.31(5), Si(1)−Fe(1)−Si(2) 141.28(5). See Supporting Information for details.

reduction. Hence, we anticipated the use of trimethylphosphine as (i) a stabilizing ligand for the expected highly electron-rich Fe(0) complex (assuming innocence of the ligand) and (ii) a labile ligand for further reactivity studies, possibly by elimination reaction.

Reduction of ***κ*^{2}*Si,Si*′-[**SiNSi**]**FeCl$_2$** with KC$_8$ in THF in the presence of an excess of PMe$_3$ indeed selectively afforded a new diamagnetic species, [**SiNSi**]**Fe(PMe$_3$)$_2$**. The C_s symmetry of the compound in solution was revealed collectively by the ^{1}H, ^{29}Si, and ^{31}P NMR spectra, all showing the inequivalency of the phosphorus atoms at the iron center (Scheme 3). The ^{1}H NMR spectrum exhibits two singlet resonances at δ = 1.09 and 1.52 ppm, two doublet signals at δ = 1.29 and 1.89 ppm, and a triplet at δ = 1.58 ppm with a relative ratio of 18:18:9:9:6, respectively. These signals were unambiguously assigned by 2D NMR experiments in the following order: the nonequivalent *tert*-butyl groups, the PMe$_3$ coligands, and the methyl group from the bound ethyl to the amine. Other aliphatic signals were observed at δ = 3.49 and 3.70 ppm, which on first inspection resembled sextets integrating for two protons each. These signals reflect the diastereotopic nature of the protons on the methylene units in the backbone. COSY ^{1}H NMR showed a correlation between both signals, and in the HSQC ^{1}H−^{13}C NMR spectra only one correlation with the methylene carbon was observed, confirming the assignment. The virtual sextet arises from the value for the $^2J_{H-H}$ coupling (14.0 Hz), being in this case exactly twice the value for the $^3J_{H-H}$ coupling (7.0 Hz).

Moreover, the C_s symmetry for the [**SiNSi**]**Fe(PMe$_3$)$_2$** complex is also consistent with the ^{31}P and ^{29}Si NMR spectra. In the former two broad signals at δ = 7.2 and 20.8 ppm highlight the inequivalency of both phosphorus atoms, and for the latter a doublet of doublets ($^2J_{Si-P}$ = 22.4 Hz, 91.9 Hz) centered at δ = 68.3 ppm showed the equivalency for both silicon atoms but with different metric coupling constants to each phosphane. The reduction of ***κ*^{2}*Ge,Ge*′-[**GeNGe**]**FeCl$_2$** by the same synthetic strategy afforded only the side products also observed during the reduction without PMe$_3$ present in the reaction. As an alternative, employing the highly reactive iron(0) precursor Fe(PMe$_3$)$_4$ in a PMe$_3$ substitution reaction with the ligand **SiNSi** at 50 °C, a new species with identical spectra to the [**SiNSi**]**Fe(PMe$_3$)$_2$** complex was observed, as seen previously using reduction with KC$_8$. Motivated by this result, we investigated the reaction between the ligand **GeNGe** and Fe(PMe$_3$)$_4$ at 50 °C, which also afforded a dark red solution after 8 h. Extraction of the crude product with pentane and removal of the solvent, followed by three freeze−pump−thaw cycles, afforded a foamy solid in high purity. Unfortunately, given the high solubility of the [**GeNGe**]**Fe(PMe$_3$)$_2$** complex in aprotic organic solvents such as pentane, hexane, diethyl ether, toluene, and THF, its crystallization was not possible. The NMR spectra exhibit signals in close analogy to the [**SiNSi**]**Fe(PMe$_3$)$_2$** complex. However, in the ^{31}P NMR spectrum two doublets at δ = 10.2 and 27.2 ppm ($^2J_{P-P}$ = 20.9 Hz) are observed instead of the broad signals for the [**SiNSi**]**Fe(PMe$_3$)$_2$** complex. This fact might be related to the

dx.doi.org/10.1021/om500966t | *Organometallics* 2014, 33, 6885−6897

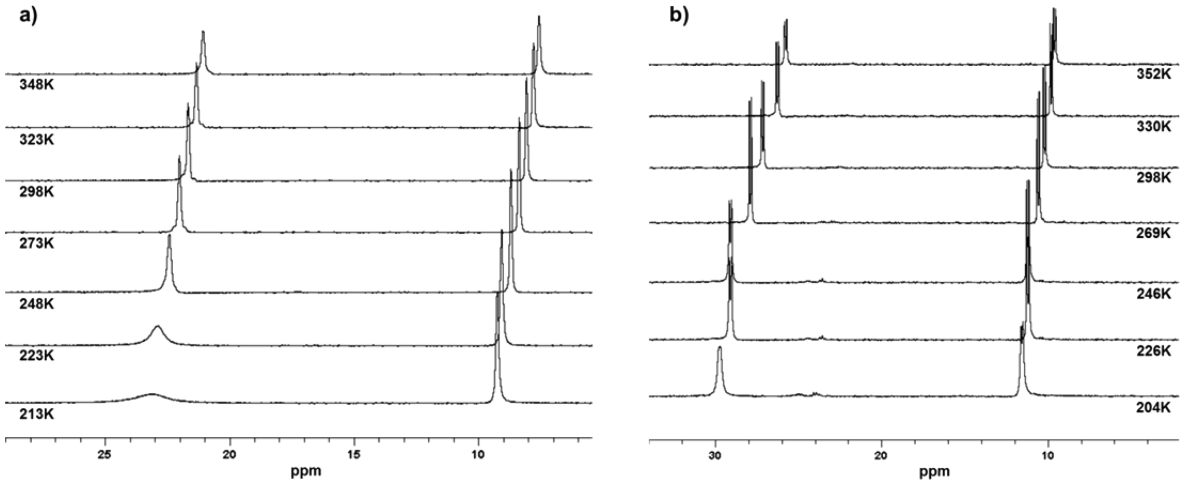

Figure 7. Stacked variable-temperature (VT) ^{31}P NMR in d_8-toluene for (a) [**SiNSi**]**Fe**($\mathbf{PMe_3}$)$_2$ and (b) [**GeNGe**]**Fe**($\mathbf{PMe_3}$)$_2$.

Berry pseudorotation rate of the phosphanes on the iron center (see VT-NMR studies below) as well as the P−Fe−P angle, as has been previously shown in other bis-phosphane metal complexes.[29]

Single crystals of [**SiNSi**]**Fe**($\mathbf{PMe_3}$)$_2$ suitable for X-ray diffraction (XRD) analysis were obtained that revealed a C_s symmetric molecule in the asymmetric unit. The geometric features of [**SiNSi**]**Fe**($\mathbf{PMe_3}$)$_2$ depict the iron center in a slightly distorted pseudo-square pyramidal (PSQP) coordination environment with τ = 0.18,[30] with a trimethylphosphine ligand occupying the apical position (Figure 6). This geometry is unusual for Fe(0) low-spin complexes,[3,31] and so a careful study was carried out to define its electronic structure (see ^{57}Fe Mössbauer spectroscopy and DFT calculations below). The apical phosphorus atom features a slightly larger bond distance to the iron center by 4.26(1) pm compared with the phosphorus atom situated at the equatorial position, and the Fe−P distances are comparable to the Fe(0) complexes with silylene as coligand of type [(dmpe)$_2$Fe(←:Si(X)L)] (L = *N,N′*-di-*tert*-butyl(phenylamidinato), X = Cl, Me, H).[17] Moreover, the Si−Fe bond distances are within the range of these complexes (2.1634−2.200 Å) and shorter when compared with the silylene→Fe(CO)$_4$ complexes reported by West (:Si(N*t*BuCH)$_2$, 2.196 Å)[32] and Roesky et al. [:Si(O*t*Bu){(N*t*Bu)$_2$CPh}], 2.237(7) Å).[33] Moreover, the bond distances are in fact comparable to the silylene→Fe complex [Cp*Fe(CO)(SiMe$_3$)SiMes$_2$] reported by Tobita and co-workers, where a formal double bond was described between the Si and Fe centers,[34] potentially indicating multiple-bonding character (see the DFT calculations below). The noninnocent behavior for the bis(imino)pyridine ligand used by Chirik and co-workers in complex **I** (Figure 1) has been demonstrated, and it is best described as an Fe(II) complex with a dianionic ligand having a radical located on each imino subunit.[4,5] This effect was previously shown to play a role in the bond distances between the metal center and the donor atoms.[4] The N−Fe bond distances in **I** can therefore be thought of as a N−Fe(II) bonding situation changing the nature of the expected N−Fe(0) bond. Recently, Milstein and co-workers[9] reported a series of dicarbonyl iron complexes stabilized by a bipyridine phosphine pincer ligand (**III** in Figure 1), where the innocent behavior of their ligand systems was demonstrated. For their examples the $N_{centered}$−Fe bond distance is shorter within a difference of 11−13 pm than in the [**SiNSi**]**Fe**($\mathbf{PMe_3}$)$_2$ complex. This difference is related with the strong Fe→CO π-back-bond. Comparisons to these well-defined complexes showed that our ligand systems most likely are innocent since bond distances are within narrow limits of actual Fe(0) complexes rather than a ligand-centered radical.

The low symmetry of the molecule in the solid state and in solution prompted us to explore the possibility whether the C_s symmetry of the unusual PSQP iron complex is simply a conformer in equilibrium with a higher (C_{2v}) symmetric system in a trigonal bipyramidal (TBP) conformation. For this purpose, variable-temperature ^{1}H and ^{31}P NMR (VT-NMR) experiments were carried out for both iron complexes [**ENE**]**Fe**($\mathbf{PMe_3}$)$_2$ (E = Si^{II}, Ge^{II}). Remarkably, the C_s symmetry remains for the entire temperature range without observing any Berry pseudorotation on the ligand system, even at rather high temperatures (Figure 7). To the best of our knowledge, these complexes therefore represent the first examples of configurationally stable PSQP Fe(0) complexes: even after heating at 70 °C for >7 days, no changes are observed. The remarkable stability of the PSQP over the TBP conformer is likely controlled by sterics: the high steric demand on the substituents on the pincer backbone likely stabilizes the iron center, thereby freezing out the trimethylphosphine coligands in the molecule.

The diamagnetic ^{1}H NMR spectrum of [**SiNSi**]**Fe**($\mathbf{PMe_3}$)$_2$ in C_6D_6 reveals exclusively signals in the diamagnetic spectral window. A clear doublet resonance at δ = 5.95 ppm corresponding to the proton at the *meta* position on the pyridine moiety and a triplet of doublets (long-range coupling $^6J_{H-P}$ = 1.77 Hz) at δ = 7.18 ppm, which corresponds to the proton at the *para* position of the pyridine backbone, are observed. This is in close agreement with the signals observed by Danopolous on pyridine in complex **II**[6] but differs substantially with the reduced bis(imino)pyridine ligand used by Chirik in complex **I**[3] (Figure 1), where large isotropic shifts were observed. This again points to the **ENE** ligands exhibiting innocent behavior, which was additionally confirmed by ^{57}Fe Mössbauer spectroscopy and DFT studies (see below).

The isomer shifts and quadrupole splitting found for the [**ENE**]**Fe**($\mathbf{PMe_3}$)$_2$ complexes in the ^{57}Fe Mössbauer spectra at 77 K (E = Si^{II}: δ = 0.24(1) mm s^{-1}, ΔE_Q = 1.66(1) mm s^{-1}; E = Ge^{II}: δ = 0.36(1) mm s^{-1}, ΔE_Q = 1.87(1) mm s^{-1}) are in the range expected for iron(0) complexes in a pentacoordinated environment (Figure 8). It is worth mentioning that these

dx.doi.org/10.1021/om500966t | *Organometallics* 2014, 33, 6885−6897

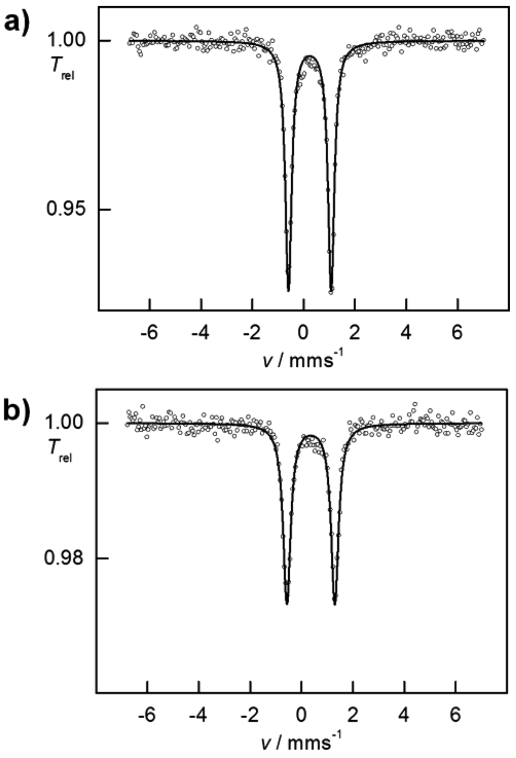

Figure 8. Zero-field ^{57}Fe Mössbauer spectra of complexes [**ENE**]**Fe**-(**PMe$_3$**)$_2$ at 77 K. The circles are experimental data, and the lines the simulated Lorentzian curves. (a) E = Si^{II}: δ = 0.24(1) mm s^{-1}, ΔE_Q = 1.66(1) mm s^{-1}, Γ_{fwhm} = 0.30 (1) mm s^{-1}. (b) E = Ge^{II}: δ = 0.36(1) mm s^{-1}, ΔE_Q = 1.87(1) mm s^{-1}, Γ_{fwhm} = 0.35(1) mm s^{-1}.

values are strongly dependent on the nature of the donor atoms and in the coordination symmetry around the iron center. Thus, a meaningful comparison can only be carried out with those iron complexes having similar structural environment (e.g., pincer moiety, pentacoordinated systems) and donor atoms (i.e., σ-donors). Table 1 shows a comparison with some reported five-coordinate iron(0) complexes with similar features to our system. Comparing the [**ENE**]**Fe(PMe$_3$)$_2$** complexes with those with PSQP structure, i.e., [PDI]Fe(N$_2$)$_2$ and [PDI]Fe(depe), the ΔE_Q is somewhat similar to the latter since the electronic structure and donor atoms are closely related to the evaluated complexes. The compounds (dmpe)$_2$Fe(:SnClAr) and (depe)$_2$FeN$_2$ bearing a TBP structure have more differentiated ΔE_Q values depending on the type of chelate ligands and donor atoms. Moreover, the dinitrogen complex [PDI]Fe(PEt$_3$)N$_2$ with a PSQP structure shows a strong effect from the dinitrogen as coligand since its value is lower than the [PDI]Fe(depe). Very recently, Chirik and co-workers extended the understanding on the electronic structure of the complex **II**, [CNC]Fe(N$_2$)$_2$ (Figure 1, Table1), synthesized by Danopoulous et al.[6] observing a redox noninnocent behavior for this bis(carbene)pyridine ligand. Therefore, the electronic structure for this complex is better described as a mixed oxidation on the Fe center (+2 and 0) with a radical located on the pyridine backbone [CNC]-Fe^0(N$_2$)$_2$ ↔ [CNC]Fe^{II}(N$_2$)$_2$.[37] Table1 shows the Mössbauer values for this complex as well as its biscarbonyl [CNC]Fe-(CO)$_2$ complex. Comparing the ΔE_Q values for these complexes and our Fe(0) complexes, there is a large difference but not with the well-defined biscarbonyl Fe(0) complexes **III**[9] (Figure 1) bearing the innocent phosphane-bipyridine PNN ligand. This points out that the electronic structures for our Fe(0) complexes are more related with the Fe(0) center rather than mixed Fe(II) ↔ Fe(0) oxidation states.

Table 1. Zero-Field Mössbauer Parameters for Iron(0) Complexes Bearing Pincer-like Phosphane and Silylene Arms

compound	δ (mm s^{-1})	ΔE_Q (mm s^{-1})	ref
[SiNSi]Fe(PMe$_3$)$_2$	0.24(1)	1.66(1)	this work
[GeNGe]Fe(PMe$_3$)$_2$	0.36(1)	1.87(1)	this work
[PDI]Fe(N$_2$)$_2$[a]	0.39	0.53	4
[PDI]Fe(depe)[b]	0.33	1.43	35
[PDI]Fe(PEt$_3$)N$_2$	0.30	1.04	35
(dmpe)$_2$Fe(:SnClAr)[c]	0.31	1.00	36
(depe)$_2$FeN$_2$	0.24	2.14	36
[PNN]Fe(CO)$_2$	0.02 (P(*t*Bu)$_2$)	1.49	9
	0.04 (P(Ph)$_2$)	1.93	
[CNC]Fe(N$_2$)$_2$[d]	0.27	0.69	37
[CNC]Fe(CO)$_2$[d]	−0.10	0.62	37

[a]Intermediate state Fe^{II} with diradical ligand PDI*. [b]depe = bis(diethylphosphino)ethane. [c]dmpe = bis(dimethylphosphino)-ethane. [d]Mixed state Fe^{II}↔Fe^0 with radical centered at the pyridine.

The δ value can be directly related to the s-electron density, thus giving insights into the oxidation state of the Fe center. For the examples shown in Table 1, the complexes bearing CO as coligands show a major influence on the isomer shifts due to the strong π-back-bonding interaction, which affects dramatically the s-electron density at the iron centers, and lower value for δ (0.02, 0.04 mm s^{-1}). For the other complexes the δ values are within the same range as for our complexes, showing their similarities on the electronic structure at the Fe center. In particular, [**SiNSi**]**Fe(PMe$_3$)$_2$** exhibits the same δ value (0.24 mm s^{-1}) as that of (depe)$_2$Fe(N$_2$), which is a good reference of a pentacoordinate Fe(0) complex. The [**GeNGe**]**Fe(PMe$_3$)$_2$** complex has a notably higher δ value (0.36 mm s^{-1}), which is related to the reduced σ-donor strength of Ge versus Si,[18,19] resulting in a lower effective s-electron density at the iron center and a concomitant increase in δ, as observed. Hence, there appears to be some correlation of the δ values for the [**ENE**]**Fe(PMe$_3$)$_2$** (E = Si^{II}, Ge^{II}) and other Fe(0) complexes with comparable ligand arrangements. In conclusion, the comparison of the ^{57}Fe Mössbauer parameters with reported values for isolated and isostructural Fe(0) and Fe(II) complexes clearly supports that the [**ENE**]**Fe(PMe$_3$)$_2$** (E = Si^{II}, Ge^{II}) compounds show similar features to other pentacooordinate Fe(0) complexes, again pointing to the innocent nature of the **ENE** ligands.

To further elucidate the electronic structure of the metal center, we conducted detailed density functional theory (DFT) calculations at the B3LYP/6-31G(d)/LANL2DZ [Fe] level of theory, to conclusively define the redox innocence/non-innocence of the ligand. We focused mostly on atomic charges from natural bond orbital (NBO) analysis and the Wiberg bond index (WBI) to define the bonding situation within a complex. A summary of the theoretical values is presented in Table 2. The bonds with the Fe center are heavily polarized according to the NBO charges on each donor atom, which is indicative of low valence (zero valence) at the Fe center. Moreover, the WBIs differ for each donor atom with the Fe center. The WBI can be considered as an underestimation of bond order in polar bonds, and the values for the Fe−Si bonds (WBI >1) therefore indicate some multiple-bonding character.[38] The molecular

dx.doi.org/10.1021/om500966t | *Organometallics* 2014, 33, 6885−6897

Table 2. NBO Charge and Wiberg Bond Index Analyses for [SiNSi]Fe(PMe$_3$)$_2$

NBO charge		Wiberg bond index	
Fe1	−1.897	Fe−Si	1.102
Si1	+1.617		1.115
Si2	+1.606	Fe−N	0.456
P1	+1.276		
P2	+1.249	Fe−P	0.808
N1	−0.458		0.857

orbitals (MOs) HOMO and HOMO−1 show the multiple-bonding character for the Fe−Si bond through a π-back-donation between the distorted $d_{x^2-y^2}$ and d_{yz} from the Fe center to the 3p orbitals from the Si(II) atoms (Figure 9). This

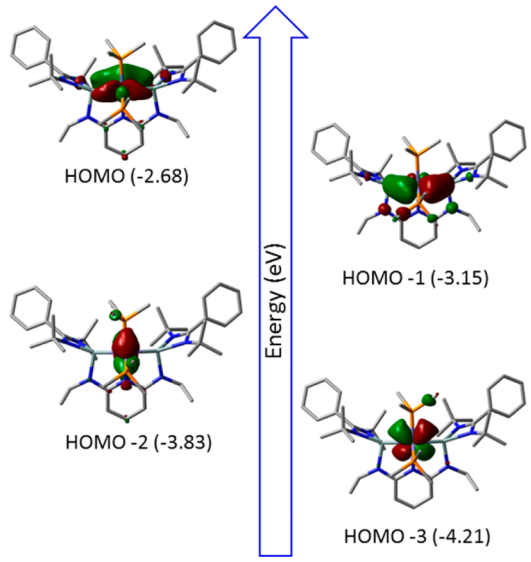

Figure 9. Selected molecular orbitals for the [SiNSi]Fe(PMe$_3$)$_2$ calculated at the B3LYP/6-31G(d)/LANL2DZ [Fe] level of theory.

is in agreement with the short Fe−Si distance in the crystal structure and comparable to our previously reported [(dmpe)$_2$Fe(←:Si(X)L)] (L = *N,N′*-di-*tert*-butyl-(phenylamidinato), X = Cl, Me, H) complexes, where a related multiple-bonding character between the Fe and Si was observed.[17] The other filled MOs, HOMO−2 and HOMO−3, are metal centered (d_{xy} and d_{xz} orbitals). It is also worth mentioning that the σ-donation from Si→Fe is observed but at lower energy (HOMO−9), where the bonding interaction is mediated by the d_{z^2} orbital from the metal center (see Supporting Information). Of importance is to note that none of the frontier orbitals show any buildup of electron density on the ligands and, thus, convincingly show that the **ENE** ligands are innocent. This is in accord with the ^{57}Fe Mössbauer spectra, the X-ray structural data, and the observed diamagnetic NMR spectra (see above).

To gain further insights into the electronic nature at the Fe(0) center in the complexes described above, we carried out the ligand substitution reactions of the [**ENE**]Fe(PMe$_3$)$_2$ complexes with CO (Figure 10) to use it as a probe in the IR spectrum. Stirring pentane solutions of the iron complexes overnight under a CO atmosphere afforded replacement of the PMe$_3$ ligands by CO. However, the reaction consistently produced a mixture of two major compounds: the disubstituted [**ENE**]Fe(CO)$_2$ and trisubstituted κ^2*E,E′*-[**ENE**]Fe(CO)$_3$, as proven by single-crystal XRD analyses (Figure 10 and Supporting Information). For the case of E = Ge^{II} another complex bearing one phosphine ligand, κ^2*Ge,Ge′*-[**GeNGe**]Fe(CO)$_2$PMe$_3$, could also be isolated. To our knowledge this reactivity of substitutionally labile pincer-type iron complexes has not been observed before for related PNP, CNC, and NNN pincer ligands, and it might again be a consequence of the strong σ-donor capacity of our novel ligand system. Therefore, in this case the higher electron density at the iron center is stabilized by the extra π-acceptor ligand CO. The high *trans* effect from the metallylenes, discussed above for the Fe(II) complexes, might favor as well the formation of the TBP iron center, having both metallylenes in a *cis* configuration at an equatorial and an apical position. These complexes, moreover, are thermally robust without observing decomposition in solutions at 70 °C after 7 days. However, after heating for 1 day, solutions containing κ^2*Ge,Ge′*-[**GeNGe**]Fe(CO)$_2$PMe$_3$ liberate PMe$_3$, through intramolecular coordination of the N atom at the pyridine backbone to iron, to give [**GeNGe**]Fe(CO)$_2$.

Table 3. Comparison of the CO Ligands in Pincer-Type Complexes by Structural and Spectroscopic Means

compound	IR ν_{CO} (cm^{-1})	XRD C−O (Å)	ref
[**SiNSi**]Fe(CO)$_2$	1830, 1778	1.192(7), 1.168(8)	this work
[**GeNGe**]Fe(CO)$_2$	1855, 1805	1.189(7), 1.164(7)	this work
[**CNC**]Fe(CO)$_2$	1928, 1865	1.161	6
[**NNN**]Fe(CO)$_2$	1974, 1914	1.147(2)	3, 39
[**PNP**]Fe(CO)$_2$	1950, 1894	1.1734(11)	39
[***i*Pr-PNN**]Fe(CO)$_2$	1895, 1838	1.1580(17), 1.1615(15)	9

The [**ENE**]Fe(CO)$_2$ complexes (E = Si^{II} and Ge^{II}) exhibit a C_{2v} symmetry in solution according to the NMR spectra, which is consistent with a TBP structure, contrary to the PSQP structure in the precursor complexes [**ENE**]Fe(PMe$_3$)$_2$. Single-crystal XRD analyses revealed that both [**ENE**]Fe(CO)$_2$ complexes (E = Si^{II} and Ge^{II}) possess a TBP structure in the solid state. The Fe−Si and Fe−N bond distances are largely invariant with the CO substitution, and the electronic structure is comparable to the [**ENE**]Fe(PMe$_3$)$_2$ complexes calculated by DFT (see Supporting Information). This additionally confirms that the unusually high stability of the PSQP structure of the [**ENE**]Fe(PMe$_3$)$_2$ complex is dominated by sterics and not by electronics at the Fe center. A summary of the bond distances and the IR stretching frequencies for the [**ENE**]Fe(CO)$_2$ pincer-type complexes is presented in Table 3. Comparing the values for the CO stretching frequencies, lower frequencies were observed for the novel [**ENE**]Fe(CO)$_2$ (E = Si^{II} and Ge^{II}) complexes as well as elongation of the C−O distance, indicating the higher σ-electron donor abilities of Si^{II} and Ge^{II} and strong Fe-CO π-back-bonding interactions. This is consistent with a more electron-rich Fe(0) center for E = Si^{II} and Ge^{II} as compared to analogous complexes with E = C^{II}, P^{III}, and N^{III} donor atoms, again pointing out the innocent behavior of these novel ligands.

Catalytic Hydrosilylation of Ketones. During the past decade iron catalysts have become widespread in several chemical transformations (e.g., hydrogenation, hydrosilylation, coupling reactions),[40] having in some examples comparable activities to their noble metal counterparts (e.g., Rh, Ir, Ru).

dx.doi.org/10.1021/om500966t | *Organometallics* 2014, 33, 6885−6897

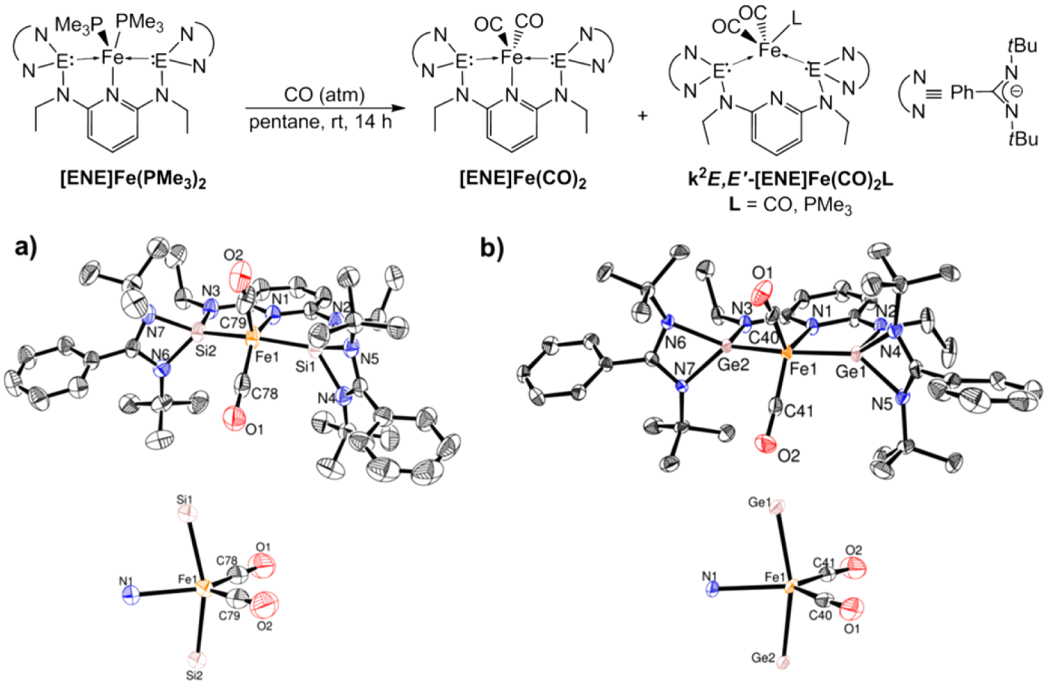

Figure 10. Ligand substitution reaction of [**ENE**]**Fe**(PMe_3)$_2$ with CO and the ORTEP representation of the [**ENE**]**Fe**(**CO**)$_2$ complexes in the solid state. Thermal ellipsoids are drawn at the 50% probability level. Hydrogen and solvent atoms are omitted for clarity. Selected distances [Å] and angles [deg]: (a) E = Si^{II}: Fe(1)−C(78) 1.701(6), Fe(1)−C(79) 1.759(7), Fe(1)−N(1) 2.089(4), Fe(1)−Si(1) 2.1579(15), Fe(1)−Si(2) 2.1664(15), Si(1)−N(2) 1.757(4), Si(1)−N(4) 1.865(5), Si(2)−N(3) 1.747(4), O(1)−C(78) 1.192(7), O(2)−C(79) 1.168(8), C(78)−Fe(1)−C(79) 114.7(3), C(78)−Fe(1)−N(1) 131.8(3), C(79)−Fe(1)−N(1) 113.5(3), C(78)−Fe(1)−Si(1) 90.85(19), C(79)−Fe(1)−Si(1) 98.33(19), N(1)−Fe(1)−Si(1) 81.36(12), C(78)−Fe(1)−Si(2) 91.82(19), C(79)−Fe(1)−Si(2) 99.49(19), N(1)−Fe(1)−Si(2) 81.33(11), Si(1)−Fe(1)−Si(2) 158.95(7). (b) E = Ge^{II}: Fe(1)−C(41) 1.718(5), Fe(1)−C(40) 1.750(6), Fe(1)−N(1) 2.156(4), Fe(1)−Ge(1) 2.2086(9), Fe(1)−Ge(2) 2.2092(9), Ge(1)−N(2) 1.880(4), Ge(1)−N(4) 1.994(4), Ge(2)−N(3) 1.870(4), O(1)−C(40) 1.164(7), O(2)−C(41) 1.189(7), C(41)−Fe(1)−C(40) 113.8(3), C(41)−Fe(1)−N(1) 126.8(2), C(40)−Fe(1)−N(1) 119.35(19), C(41)−Fe(1)−Ge(1) 97.06(17), C(40)−Fe(1)−Ge(1) 93.56(16), N(1)−Fe(1)−Ge(1) 82.06(11), C(41)−Fe(1)−Ge(2) 90.51(17), C(40)−Fe(1)−Ge(2) 96.20(16), N(1)−Fe(1)−Ge(2) 82.15(11), Ge(1)−Fe(1)−Ge(2) 164.04(4). See Supporting Information for details.

Scheme 4. Proof of Catalytic Activity of Iron(0) Complex [SiNSi]Fe(PMe_3)$_2$ as a Precatalyst in the Hydrosilylation of Acetophenone Derivatives

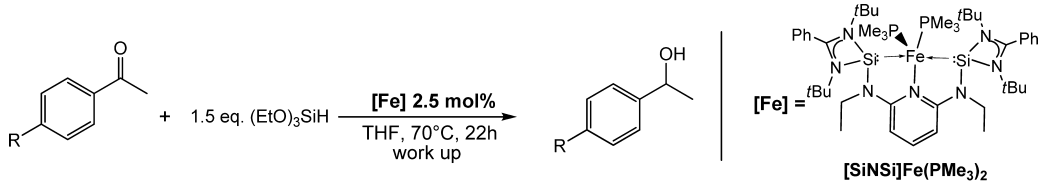

R	H	OMe	Me	Br	CF_3
Yield (%)	93	>99	82	>99	95

Several iron pincer-type complexes have shown to be very robust under different catalytic conditions as well as very active even under mild conditions.[14−16] Consequently, we were interested to probe the ability of the obtained iron(0) complexes for the catalytic hydrosilylation of a ketone. Previously, we reported the hydrosilylation of ketones employing the [(dmpe)$_2$Fe(←:Si(H)L)] (L = *N,N′*-di-*tert*-butyl(phenylamidinato)) complex, where a cooperative behavior was elucidated between the silicon(II) and iron(0) centers.[17] This result demonstrated that a silylene can act as a cooperative ligand in catalytic systems. However, an innocent silylene ligand would also be of interest when a robust catalyst is required. In preliminary experiments employing catalytic amounts (2 mol %) of the [**SiNSi**]**Fe**(PMe_3)$_2$ complexes in the hydrosilylation of *p*-methoxyacetophenone with triethoxysilane, we obtained conversions up to 87% after 22 h at 70 °C in THF (see Supporting Information). After the catalytic run a clear orange solution resulted without observable decomposition of the catalytic system. Increasing the precatalyst loading to 2.5 mol %, a quantitative yield could be obtained for *p*-methoxyacetophenone as well as for other ketones as substrates (Scheme 4) in which the catalytic activity is somehow improved to our previous system where a catalyst loading of 5 mol % was required under the same catalytic conditions.[17] Currently we are varying the catalytic conditions and extending the substrate scope to understand the mechanism for this chemical transformation.

dx.doi.org/10.1021/om500966t | *Organometallics* 2014, 33, 6885−6897

CONCLUSIONS

In summary, the first bis(silylene)- and bis(germylene)-pyridine [**ENE**] (E = Si^{II}, Ge^{II}) pincer ligands were synthesized by a salt metathesis reaction of the dilithiated 2,6-bis(ethylamino)-pyridine and with amidinato-stabilized chlorosilylene or chlorogermylene. The novel [**ENE**] ligands behave in an innocent fashion on coordination to iron, as shown by a range of spectroscopic, structural, and theoretical investigations, in contrast to many other previously reported pincer-type iron complexes, which usually show ligand-centered radical ground-state configurations. The iron complexes κ^2***E,E′*-[ENE]$FeCl_2$** were synthesized by direct coordination of $FeCl_2$, affording tetrahedral iron(II) complexes lacking coordination through the N atom at the pyridine backbone according to single-crystal XRD, ^{57}Fe Mössbauer, and magnetometric measurements. Either by reduction of the κ^2***Si,Si′*-[SiNSi]$FeCl_2$** with KC_8 in the presence of PMe_3 or by a direct substitution reaction of the iron(0) precursor $Fe(PMe_3)_4$ with the **ENE** pincer ligands the unusual electron-rich **[ENE]Fe$(PMe_3)_2$** complexes with Fe(0) sites are accessible. Remarkably, these complexes exist in a pseudo-square-pyramidal ground-state structure, which is configurationally stable over a wide range of temperatures in solution. A direct comparison with the dicarbonyl **[ENE]Fe$(CO)_2$** complexes, featuring the more expected trigonal bipyramidal structure and (pyridine)N→Fe coordination, showed that this stability is controlled by sterics since the structural features and DFT calculations demonstrated that the electronic situation on the iron center remains unchanged in both complexes with either PMe_3 or CO as coligands. Also, a comparison with the well-established pyridine-based iron complexes bearing pincer-like ligands with phosphines, carbenes, or imino groups revealed that the novel **[ENE]Fe$(PMe_3)_2$** complexes are the most electron-rich pincer-like iron(0) complexes reported to date, due to the increased σ-donor properties of the **ENE** ligands. Finally, the **[SiNSi]Fe$(PMe_3)_2$** complex showed good catalytic activity when employed as a precatalyst for the hydrosilylation of acetophenones, this being the second generation of silylene-iron-based catalysts for this type of chemical transformation. We are currently investigating the scope of substrates and the mechanism of the ketone hydrosilylation reaction and will present these results in due course.

EXPERIMENTAL SECTION

General Considerations. All experiments and manipulations were conducted under dry, oxygen-free nitrogen using standard Schlenk techniques or in a MBraun drybox with an atmosphere of purified nitrogen. Solvents were dried by standard methods and freshly distilled prior to use. ^{1}H, ^{13}C, ^{31}P, and ^{29}Si NMR spectra were recorded on Bruker AV 400 (^{1}H, 400.13 MHz; ^{13}C, 100.61 MHz; ^{29}Si, 79.49 MHz; ^{31}P, 161.80 MHz) or AFM 200 (^{1}H, 200.13 MHz; ^{13}C, 50.32 MHz; ^{31}P, 81.01 MHz) spectrometers. The NMR signals are reported relative to the residual solvent peaks (^{1}H, C_6D_6, 7.15 ppm; C_7D_8, 2.09 ppm; $CDCl_3$, 7.26 ppm; ^{13}C, C_6D_6, 128.0 ppm; C_7D_8, 20.4 ppm; $CDCl_3$, 77.2 ppm) or an external standard (^{31}P, 85% H_3PO_4, 0.0 ppm; ^{29}Si, TMS, 0.0 ppm). All signals were unambiguously assigned by a combination of 2D NMR H−H COSY, HSQC, and HMBC correlation spectroscopy. Mass spectra were recorded using APCI or ESI as ionization source and an LTQ Orbitrap XL as analyzer. Elemental analyses were recorded in a Thermo FlashEA 1112 Organic elemental analyzer. IR spectra were recorded on a PerkinElmer Spectrum 100 FT-IR. GC-MS measurements were conducted on a Shimadzu GC-2010 gas chromatograph (30 m Rxi-5 ms column) linked to a Shimadzu GCMA-QP 2010 Plus mass spectrometer. The $FeCl_2$, PMe_3, and $(EtO)_3SiH$ were purchase from Sigma Aldrich and used as received. The *N,N′*-di-*tert*-butyl(phenylamidinato)-chlorosilylene,[41] *N,N′*-di-*tert*-butyl(phenylamidinato)-chlorogermylene,[42] and $Fe(PMe_3)_4$[43] were prepared according to the reported procedures.

Single-Crystal X-ray Structure Determinations. Crystals were mounted on a glass capillary in perfluorinated oil and measured in a cold N_2 flow. The data were collected either on an Agilent Technologies Xcalibur S Sapphire at 150 K (Mo Kα radiation, λ = 0.710 73 Å) or on an Agilent Technologies SuperNova (single source) at 150 K (Cu Kα radiation, λ = 1.5418 Å). The structures were solved by direct methods and refined on F^2 with the SHELX-97 software package.[44] The positions of the H atoms were calculated and considered isotropically according to a riding model.

Synthesis of 2,6-Diamine-*N,N′*-diethylpyridine. The synthesis was carried out following a reported procedure for reduction of diamides with LAH in THF under reflux.[20−22] A 5.29 g (0.027 mol) amount of the *N,N′*-diacetyl-2,6-diamidopyridine was dissolved in 60 mL of THF and dropwise added into a suspension of 6.56 g (0.173 mol) of LAH in 40 mL of THF at 0 °C. After stirring for 1 h at room temperature the reaction was refluxed overnight until completion of the reaction controlled by GC-MS. The excess of LAH was quenched at 0 °C with a basic KOH 5% solution, obtaining two phases. The phases were separated, and the aqueous phase was treated with diethyl ether (3 × 30 mL). All organic fractions were collected and dried with Na_2SO_4. Filtration and removal of all volatiles *in vacuo* afforded the product in high purity as a yellow oil (3.5 g, 77% yield). ^{1}H NMR (200.13 MHz, $CDCl_3$, 298 K): δ(ppm) = 1.22 (t, 6H, $^3J_{H-H}$ = 7.16 Hz, CH_3), 3.21 (q, 2H, $^3J_{H-H}$ = 7.16 Hz, CH_2), 3.24 (q, 2H, $^3J_{H-H}$ = 7.16 Hz, CH_2), 5.70 (d, 2H, $^3J_{H-H}$ = 7.91 Hz, 3,5-H py), 7.24 (t, 1H, $^3J_{H-H}$ = 7.91 Hz, 4-H py). ^{13}C{^{1}H} NMR (50.32 MHz, $CDCl_3$, 298 K): δ(ppm) = 15.0 (CH_3), 36.9 (CH_2), 94.39 (3,5-CH py), 139.0 (4-CH py), 158.3 (2-*C* py). ESI-MS (*m*/*z*): calcd for [$C_9H_{15}N_3$ + H^+] 166.13387; found 166.13379 (correct isotope pattern).

Synthesis of the Pincer-Type Ligand SiNSi. A 6.40 mL sample of *n*-BuLi, 1.6 M in hexanes (10.2 mmol), was added rapidly to a 30 mL diethyl ether solution of 2,6-*N,N′*-diethylaminopyridine (0.847 g, 5.13 mmol) at −30 °C, forming a yellowish solution. After warming to room temperature it was refluxed for 3 h. The resulting orange solution was cooled to −78 °C, and a solution of *N,N′*-di-*tert*-butyl(phenylamidinato)chlorosilylene (3.019 g, 10.2 mmol) in 30 mL of toluene was dropwise added via cannula. The color changed with the addition to dark red. All volatiles were removed *in vacuo* after stirring overnight, with slow warming to room temperature. The product was extracted with 60 mL of hexanes at 60 °C via cannula filtration. The solution was concentrated to 10 mL and crystallized at −30 °C over 3 days, affording large yellow crystals. Further filtration and drying produced 2.90 g of the desired product (90% yield). Suitable crystals for X-ray diffraction analysis were grown in a concentrated hexane solution at 0 °C after 2 days. ^{1}H NMR (400.13 MHz, C_6D_6, 298 K): Symmetric conformer: δ(ppm) = 1.16 (s, 36H, $NC(CH_3)_3$), 1.63 (t, $^3J_{H-H}$ = 6.9 Hz, 6H, NCH_2-CH_3), 3.77 (q, $^3J_{H-H}$ = 6.9 Hz, 4H, NCH_2-CH_3), 6.87−7.09 (m, 10H, arom. C-H), 7.34−7.50 (m, 3H, arom. C-H py). Asymmetric conformer: δ(ppm) = 1.14 (s, 36H, $NC(CH_3)_3$), 1.55 and 1.68 (t, $^3J_{H-H}$ = 6.9 Hz, 6H, NCH_2-CH_3), 3.71 and 4.62 (q, $^3J_{H-H}$ = 6.9 Hz, 4H, NCH_2-CH_3). ^{13}C{^{1}H} NMR (100.61 MHz, C_6D_6, 298 K): Symmetric conformer: δ(ppm) = 16.9 (NCH_2-CH_3), 31.6 ($NC(CH_3)_3$), 31.9 (NCH_2-CH_3), 52.9 ($NC(CH_3)_3$), 101.8 (3,5-C_{arom} py), 127.6 (C_{arom}), 128.5 (C_{arom}), 129.3 (C_{arom}), 129.3 (C_{arom}), 129.4 (C_{arom}), 130.0 (C_{arom}), 130.5 (C_{arom}), 130.5 (C_{arom}), 134.7 (C_{arom} quaternary Ph), 136.9 (4-C_{arom} py), 161.2 (2,6-C_{arom} py), 161.4 (NCN). Asymmetric conformer: δ(ppm) = 18.0 and 16.0 (NCH_2-CH_3), 31.4 and 31.5 ($NC(CH_3)_3$), 36.8 and 43.9 (NCH_2-CH_3), 53.3 ($NC(CH_3)_3$), 103.0 and 103.9 (3,5-C_{arom} py), 134.0 and 134.5 (C_{arom} quaternary Ph), 136.4 (4-C_{arom} py). ^{29}Si{^{1}H} NMR (79.49 MHz, C_6D_6, 298 K): Symmetric conformer: δ(ppm) = −14.9. Asymmetric conformer: δ(ppm) = −13.8 and −17.1. APCI-MS (*m*/*z*): calcd for [($C_{39}H_{59}N_7Si_2$+OH)$^{\bullet+}$] 698.43924; found 698.43983 (correct isotope pattern).

dx.doi.org/10.1021/om500966t | *Organometallics* 2014, 33, 6885−6897

Synthesis of the Pincer-Type Ligand GeNGe. The synthesis of the bis(germylene)pyridine pincer ligand proceeded in a similar fashion to that for the synthesis of the pincer ligand **SiNSi** (see above). After the addition of the *N,N′*-di-*tert*-butyl(phenylamidinate)-chlorogermylene (1.788 g, 5.27 mmol) in 30 mL of toluene the color of the reaction mixture changed to an intense yellowish solution. All volatiles were removed *in vacuo* after stirring overnight, warming to room temperature with the cold bath. The product was extracted with 60 mL of hexanes at 60 °C for 1 h via cannula filtration. Removal of the solvent produced 1.98 g of a yellowish foamy solid with high purity according to the NMR spectra (98% yield). ^{1}H NMR (400.13 MHz, C_6D_6, 298 K): δ(ppm) = 1.11 (s, 36H, NC(CH_3)$_3$), 1.53 (t, $^{3}J_{H-H}$ = 7.0 Hz, 6H, NCH_2-CH_3), 3.76 (q, $^{3}J_{H-H}$ = 7.0 Hz, 4H, NCH_2-CH_3), 6.34 (d, $^{3}J_{H-H}$ = 7.9 Hz, 2H, 3,5-H py), 6.88−7.11 (m, 10H, arom. C-H Ph), 7.46 (t, $^{3}J_{H-H}$ = 7.9 Hz, 1H, 4-H py). ^{13}C{^{1}H} NMR (100.61 MHz, C_6D_6, 298 K): δ(ppm) = 16.8 (NCH_2-CH_3), 32.2 (NC(CH_3)$_3$), 38.8 (NCH_2-CH_3), 52.8 (NC(CH_3)$_3$), 95.2 (3,5-C_{arom} py), 127.5 (C_{arom}), 128.9 (C_{arom}), 130.3 (C_{arom}), 136.9 (C_{arom} quaternary Ph), 138.7 (4-C_{arom} py), 162.6 (2,6-C_{arom} py), 167.3 (NCN). APCI-MS (*m*/*z*): calcd for [$C_{39}H_{59}Ge_2N_7^{\bullet+}$] 773.32500; found 773.32666 (correct isotope pattern). Anal. Calcd for $C_{39}H_{59}Ge_2N_7$: calcd, C 60.74, H 7.71, N 12.71; found C 60.47, H 7.72, N 12.40.

Synthesis of [ENE]FeCl$_2$ (E = Si^{II}, Ge^{II}) Complexes. A suspension of $FeCl_2$ (1.1 equiv) was heated in 30 mL of THF at 60 °C for 2 h. After cooling to room temperature, a solution of **ENE** (1.0 equiv) in 20 mL of THF was dropwise added via cannula, dissolving all suspended solid. After stirring at room temperature for 3 h, all volatiles were removed under vacuum, forming a yellowish solid. The product was extracted with toluene (1 × 60 mL, 1 × 30 mL) and filtered off via cannula. Concentration *in vacuo* to 10 mL and crystallization at −30 °C afforded the desired product as yellow crystals.

Complex [SiNSi]FeCl$_2$. At 1.0 mmol scale: 73% yield; yellow blocks. Suitable crystals for X-ray diffraction analysis were grown from a concentrated toluene solution at 0 °C after 3 days. ^{1}H NMR paramagnetic (200.13 MHz, C_6D_6, 298 K): δ(ppm) = −2.25 (36H), 1.24 (6H), 2.80 (2H), 5.61 (2H), 6.53 (2H), 10.29 (1H), 10.66 (2H), 13.32 (2H), 21.83 (4H), 24.41 (2H). Evans (C_6D_6, tetramethylsilylsilane capillary, concentration 0.031 g mL^{-1}, 200 MHz for ^{1}H): μ_{eff} = 4.65 μ_B. ^{57}Fe Mössbauer at 77 K (zero field): δ = 0.73(1) mm s^{-1}, ΔE_Q = 3.06(1) mm s^{-1}, Γ_{fwhm} = 0.34(1) mm s^{-1}. APCI-MS (*m*/*z*): calcd for [$C_{39}H_{59}Cl_2FeN_7Si_2^{\bullet+}$] 807.30915; found 807.30914 (correct isotope pattern). Anal. Calcd for $C_{39}H_{59}Cl_2FeN_7Si_2{\cdot}C_7H_8$: C 61.32, H 7.50, N 10.88. Found: C 59.61, H 7.58, N 10.99.

Complex [GeNGe]FeCl$_2$. At 1.0 mmol scale: 83% yield; yellow blocks. Suitable crystals for X-ray diffraction analysis were grown from a concentrated toluene solution at −78 °C after 3 days. ^{1}H NMR paramagnetic (200.13 MHz, C_6D_6, 298 K): δ(ppm) = −0.11 and 0.36 (two signals overlapping, 36H), 1.00−1.42 (5H), 3.29 (2H), 4.90 (2H), 5.17 (1H), 5.95 (2H), 8.06 (2H), 8.86 (2H), 11.93 (1H), 26.70 (4H). Evans (C_6D_6, tetramethylsilylsilane capillary, concentration 0.029 g mL^{-1}, 200 MHz for ^{1}H): μ_{eff} = 4.71 μ_B. ^{57}Fe Mössbauer at 77 K (zero field): δ = 0.82(1) mm s^{-1}, ΔE_Q = 2.57(1) mm s^{-1}, Γ_{fwhm} = 0.46(1) mm s^{-1}. APCI-MS (*m*/*z*): calcd for [$C_{39}H_{59}Cl_2FeGe_2N_7^{\bullet+}$] 899.19765; found 899.19928 (low intensity); calcd for [($C_{39}H_{59}Cl_2FeGe_2N_7$ − Cl)$^+$] 864.22935; found 864.38190 (correct isotope pattern). Anal. Calcd for $C_{39}H_{59}Cl_2FeGe_2N_7{\cdot}C_7H_8$: C 55.80, H 6.82, N 9.90. Found: C 55.06, H 7.01, N 10.20.

Synthesis of [SiNSi]Fe(PMe$_3$)$_2$ Complex. Method A: A strong yellow solution of [**SiNSi**]**FeCl$_2$** (414 mg, 0.511 mmol) in 30 mL of THF was dropwise added via cannula to a Schlenk flask containing KC_8 (220 mg, 1.63 mmol) at −10 °C. After 15 min stirring, a solution of PMe_3 (1.0 M in hexanes) (2.0 mL, 2.0 mmol) was added dropwise via syringe with a change in color to red. After warming to room temperature and 24 h stirring, the reaction mixture had a dark purple color. The solution was filtered via cannula, and all volatiles were removed *in vacuo*, producing a sticky purple solid. The product was extracted with pentane (1 × 50 mL, 1 × 20 mL) and concentrated *in vacuo*, affording 350 mg (77% yield) of a purple solid after three freeze−thaw cycles in high purity according to the NMR spectra. Suitable crystals for X-ray diffraction analysis were grown in a concentrated pentane solution at 0 °C after ca. 1 week. Method B: A solution of **SiNSi** (160 mg, 0.235 mmol) in 10 mL of hexane was dropwise added to a solution of Fe(PMe_3)$_4$ (85 mg, 0.24 mmol) in 10 mL of hexane at room temperature. The mixture was warmed to 50 °C for 8 h under continuous stirring. The solvent was pumped off and the product extracted with 40 mL of pentane. Concentration, crystallization, filtration, and drying *in vacuo* afforded 100 mg of the desired product (48% yield). ^{1}H NMR (200.13 MHz, C_6D_6, 298 K): δ(ppm) = 1.09 (s, 18H, 2 × NC(CH_3)$_3$), 1.29 (d, 9H, $^{2}J_{H-P}$ = 4.0 Hz, $P_A(CH_3)_3$), 1.52 (s, 18H, 2 × NC(CH_3)$_3$), 1.58 (t, 6H, $^{3}J_{H-H}$ = 7.0 Hz, NCH′H-CH_3), 1.89 (d, 9H, $^{2}J_{H-P}$ = 4.0 Hz, $P_B(CH_3)_3$), 3.49 (virtual sextet with roof effect, 2H, $^{2}J_{H-H}$ = 14.0 Hz, $^{3}J_{H-H}$ = 7.0 Hz, NCH′*H*-CH_3), 3.70 (virtual sextet with roof effect, 2H, $^{2}J_{H-H}$ = 14.0 Hz, $^{3}J_{H-H}$ = 7.0 Hz, NC*H*′H-CH_3), 6.04 (d, 2H, $^{3}J_{H-H}$ = 7.7 Hz, 3−5-H py), 6.96−7.06 (m, 6H, arom. C-H), 7.19−7.27 (m, 3H, arom. C*H* and 4-H py), 7.42−7.51 (m, 2H, arom. C*H*). ^{1}H NMR (400.13 MHz, C_7D_8, 298 K): δ(ppm) = 1.07 (s, 18H, 2 × NC(CH_3)$_3$), 1.21 (d, 9H, $^{2}J_{H-P}$ = 4.4 Hz, $P^A(CH_3)_3$), 1.51 (s, 18H, 2 × NC(CH_3)$_3$), 1.56 (t, 6H, $^{3}J_{H-H}$ = 7.0 Hz, NCH′H-CH_3), 1.83 (d, 9H, $^{2}J_{H-P}$ = 6.1 Hz, $P^B(CH_3)_3$), 3.46 (virtual sextet with roof effect, 2H, $^{2}J_{H-H}$ = 14.0 Hz, $^{3}J_{H-H}$ = 7.0 Hz, NCH′*H*-CH_3), 3.69 (virtual sextet with roof effect, 2H, $^{2}J_{H-H}$ = 14.0 Hz, $^{3}J_{H-H}$ = 7.0 Hz, NC*H*′H-CH_3), 5.95 (d, 2H, $^{3}J_{H-H}$ = 8.0 Hz, 3−5-H py), 7.18 (td, 1H, $^{3}J_{H-H}$ = 8.0 Hz, $^{6}J_{H-P}$ = 1.8 Hz, 4-H py), 6.99−7.08 (m, 6H, arom. C*H*), 7.24−7.28 (m, 2H, arom. C*H*), 7.44−7.48 (m, 2H, arom. C*H*). ^{13}C{^{1}H} NMR (100.61 MHz, C_7D_8, 298 K): δ(ppm) = 15.6 (NCH_2-CH_3), 25.9 (d, $^{1}J_{C-P}$ = 10.8 Hz, $P_A(CH_3)_3$), 33.9 (dd, $^{1}J_{C-P}$ = 13.07 Hz, $^{3}J_{C-P}$ = 5.60 Hz, P(CH_3)$_3$), 31.6 (NC(CH_3)$_3$), 33.3 (NC(CH_3)$_3$), 38.9 (NCH_2−CH_3), 53.3 (NC(CH_3)$_3$), 53.5 (NC(CH_3)$_3$), 93.3 (d, $^{4}J_{C-P}$ = 2.20 Hz, 3,5-C_{arom} py), 126.6 (d, $^{5}J_{C-P}$ = 3.26 Hz, 2,6-C_{arom} py), 127.3 (C_{arom}), 127.4 (C_{arom}), 130.5 (C_{arom}), 135.3 (C_{arom} quaternary Ph), 165.3 (d, $^{3}J_{C-P}$ = 3.26 Hz, 2,6-C_{arom} py), 168.5 (NCN). ^{29}Si{^{1}H} NMR (79.49 MHz, C_7D_8, 298 K): 68.3 (dd, $^{2}J_{Si-P}$ = 22.40 Hz, 91.87 Hz, Si:). ^{31}P NMR (161.97 MHz, C_7D_8, 298 K): 7.2 (bs, *P*Me_3), 20.8 (bs with satellites $^{2}J_{P-Si}$ = 91.87 Hz, *P*Me_3). ^{57}Fe Mössbauer at 77 K (zero field): δ = 0.24(1) mm s^{-1}, ΔE_Q = 1.66(1) mm s^{-1}, Γ_{fwhm} = 0.30 (1) mm s^{-1}. APCI-MS (*m*/*z*): calcd for [$C_{45}H_{77}FeN_7P_2Si_2^{\bullet+}$] 889.45982; found 889.45978 (correct isotope pattern).

Synthesis of [GeNGe]Fe(PMe$_3$)$_2$ Complex. The synthesis of this complex was ONLY affordable by method B described above for [**SiNSi**]**Fe(PMe$_3$)$_2$** complex. Extraction with pentane and removal of the solvent *in vacuo* afforded a foamy-like dark red solid in high purity. At 0.5 mmol scale: 90% yield. ^{1}H NMR (400.13 MHz, C_6D_6, 298 K): δ(ppm) = 1.08 (s, 18H, 2 × NC(CH_3)$_3$), 1.29 (d, $^{2}J_{H-P}$ = 5.33 Hz, 9H, $P_A(CH_3)_3$), 1.47 (s, 18H, 2 × NC(CH_3)$_3$), 1.57 (t, $^{3}J_{H-H}$ = 7.04 Hz, 6H, NCH′H-CH_3), 1.76 (d, $^{2}J_{H-P}$ = 6.62 Hz, 9H, $P_B(CH_3)_3$), 3.76 ("sextet" with roof effect, $^{2}J_{H-H}$ = 13.98 Hz, $^{3}J_{H-H}$ = 6.99 Hz, 2H, NCH′*H*-CH_3), 3.95 ("virtual sextet" with roof effect, $^{2}J_{H-H}$ = 13.98 Hz, $^{3}J_{H-H}$ = 6.99 Hz, 2H, NC*H*′H-CH_3), 6.00 (d, $^{3}J_{H-H}$ = 7.93 Hz, 2H, 3,5-H py), 6.97−7.05 (m, 6H, arom. C-H), 7.22−7.29 (m, 3H, arom. C-H and 4-H py), 7.33−7.39 (m, 2H, arom. C-H). ^{1}H NMR (400.13 MHz, C_7D_8, 298 K): δ(ppm) = 1.06 (s, 18H, 2 × NC(CH_3)$_3$), 1.23 (d, $^{2}J_{H-P}$ = 5.33 Hz, 9H, $P_A(CH_3)_3$), 1.46 (s, 18H, 2 × NC(CH_3)$_3$), 1.56 (t, $^{3}J_{H-H}$ = 6.99 Hz, 6H, NCH′H-CH_3), 1.73 (d, $^{2}J_{H-P}$ = 7.04 Hz, 9H, $P_B(CH_3)_3$), 3.73 ("virtual sextet" with roof effect, $^{2}J_{H-H}$ = 13.98 Hz, $^{3}J_{H-H}$ = 6.99 Hz, 2H, NCH′*H*-CH_3), 3.93 ("virtual sextet" with roof effect, $^{2}J_{H-H}$ = 13.98 Hz, $^{3}J_{H-H}$ = 6.99 Hz, 2H, NC*H*′H-CH_3), 5.93 (d, $^{3}J_{H-H}$ = 7.92 Hz, 2H, 3,5-H py), 7.16 (t, $^{3}J_{H-H}$ = 7.92 Hz, 1H, 4-H py), 7.03−7.08 (m, 6H, arom. C-H), 7.27−7.32 (m, 2H, arom. C-H), 7.35−7.40 (m, 2H, arom. C-H). ^{13}C NMR (100.61 MHz, C_7D_8, 298 K): δ(ppm) = 16.0 (NCH_2-CH_3), 25.4 (d, $^{1}J_{C-P}$ = 14.4 Hz, P(CH_3)$_3$), 32.9 (NC(CH_3)$_3$), 33.3 (dd, $^{1}J_{C-P}$ = 15.9 Hz, $^{3}J_{C-P}$ = 3.7 Hz, P(CH_3)$_3$), 33.4 (NC(CH_3)$_3$), 40.5 (NCH_2-CH_3), 53.7 (NC(CH_3)$_3$), 91.7 (d, $^{4}J_{C-P}$ = 1.4 Hz, 3,5-C_{arom} py), 127.3 (C_{arom}), 127.5 (C_{arom}), 128.4 (d, $^{5}J_{C-P}$ = 3.3 Hz, 4-C_{arom} py), 130.6 (C_{arom}), 137.0 (C_{arom} quaternary Ph), 164.1 (d, $^{3}J_{C-P}$ = 2.1 Hz, 2,6-C_{arom} py), 169.0 (NCN). ^{31}P{^{1}H} NMR (161.97 MHz, C_7D_8, 298 K): δ(ppm) = 10.2 (d, $^{2}J_{P-P}$ = 20.8 Hz, *P*Me_3), 27.2 (d, $^{2}J_{P-P}$ = 20.8 Hz, *P*Me_3). ^{57}Fe Mössbauer at 77 K (zero field): δ = 0.36(1) mm s^{-1}, ΔE_Q

dx.doi.org/10.1021/om500966t | *Organometallics* 2014, 33, 6885−6897

= 1.87(1) mm s^{-1}, Γ_{fwhm} = 0.35(1) mm s^{-1}. APCI-MS (m/z): calcd for [($C_{45}H_{77}FeGe2N_7P_2$-2PMe_3)$^{\bullet+}$] 827.26139; found 827.26380 (correct isotope pattern).

Synthesis of [SiNSi]Fe(CO)$_2$ Complex. A solution of [**SiNSi**]-**Fe(PMe$_3$)$_2$** (79 mg, 0.089 mmol) in 20 mL of pentane was set up under a CO atmosphere after 3 freeze−pump−thaw cycles. The reaction mixture was stirred overnight, affording an orange solid in suspension with an orange solution. The solid was filtered off by cannula and dried *in vacuo*, affording a first crop of the desired product in high purity (40 mg). Concentration, crystallization, filtration, and drying *in vacuo* of the remaining solution in pentane afforded the second crop of the product (20 mg) for a total yield of 60 mg of the product (85% yield). ^{1}H NMR (400.13 MHz, C_6D_6, 298 K): δ(ppm) = 1.39 (s, 36H, 4 × NC(CH_3)$_3$), 1.39 (t, overlapping with singlet at 1.39 ppm, 6H, NCH′H-CH_3), 3.52 (q, $^3J_{H-H}$ = 7.1 Hz, 4H, NCH'H-CH_3), 6.18 (d, $^3J_{H-H}$ = 8.0 Hz, 2H, 3,5-H py), 6.81−7.06 (m, 10H, arom. C-H), 7.31 (t, $^3J_{H-H}$ = 8.0 Hz, 1H, 4-H py). ^{13}C{^{1}H} NMR (100.61 MHz, C_6D_6, 298 K): δ(ppm) = 15.2 (NCH_2-CH_3), 31.1 (NC(CH_3)$_3$), 38.9 (NCH_2-CH_3), 54.6 (NC(CH_3)$_3$), 95.8 (3,5-C_{arom} py), 127.3 (C_{arom}), 129.7 (C_{arom}), 129.7 (C_{arom}), 130.9 (4-C_{arom} py), 132.4 (C_{arom} quaternary Ph), 165.0 (2,6-C_{arom} py), 172.3 (NCN), 222.0 (CO). ^{29}Si{^{1}H} NMR (79.49 MHz, C_6D_6, 298 K): δ(ppm) = 98.3. IR (KBr pellet): ν_{CO}(cm^{-1}) = 1830, 1778. APCI-MS (m/z): calcd for [$C_{41}H_{59}FeN_7O_2Si_2^{\bullet+}$] 793.36127; found 793.36353.

Synthesis of [GeNGe]Fe(CO)$_2$ Complex. The synthesis for this complex was carried out in a fashion similar to the synthesis of [**SiNSi**]**Fe(CO)$_2$** described previously. At 0.11 mmol scale. [**GeNGe**]-**Fe(CO)$_2$**: 39% yield. ^{1}H NMR (400.13 MHz, C_6D_6, 298 K): δ(ppm) = 1.26 (s, 36H, NC(CH_3)$_3$), 1.39 (t, $^3J_{H-H}$ = 6.8 Hz, 6H, NCH′H-CH_3), 3.71 (q, $^3J_{H-H}$ = 6.8 Hz, 4H, NCH'H-CH_3), 6.24 (d, $^3J_{H-H}$ = 8.0 Hz, 2H, 3.5-H py), 6.86−7.05 (m, 10H, arom. C-H), 7.34 (t, $^3J_{H-H}$ = 8.0 Hz, 1H, 4-H py). ^{13}C{^{1}H} NMR (100.61 MHz, C_6D_6, 298 K): δ(ppm) = 15.5 (NCH_2-CH_3), 31.4 (NC(CH_3)$_3$), 40.5 (NCH_2-CH_3), 54.8 (NC(CH_3)$_3$), 94.9 (3,5-C_{arom} py), 127.3 (C_{arom}), 129.4 (C_{arom}), 129.7 (C_{arom}), 132.1 (4-C_{arom} py), 133.7 (C_{arom} quaternary Ph), 162.8 (2,6-C_{arom} py), 172.0 (NCN), 220.6 (CO). IR (KBr pellet) ν_{CO}(cm^{-1}) = 1855, 1805. ESI-MS (m/z): calcd for [$C_{41}H_{59}FeGe_2N_7O_2^{\bullet+}$] 883.25067; found 883.25446. [**GeNGe**]**Fe(CO)$_3$**: 30% yield. IR (KBr pellet) ν_{CO}(cm^{-1}) = 1956, 1883, 1869.

Catalytic Hydrosilylation of Acetophenones. In a nitrogen-filled drybox, [**SiNSi**]**Fe(PMe$_3$)$_2$** (2.5 mol %, 2.5 μmol), ketone (0.10 mmol), and (EtO)$_3$SiH (0.15 mmol) were weighed in a Schlenk flask containing a stir bar and dissolved in 2 mL of THF. The flask was taken out of the drybox, stirred, and heated to 70 °C in an oil bath for 22 h. The reaction mixture was treated with an aqueous potassium hydroxide solution (2 mL, 5%) and stirring. The reaction mixture was stirred for 2 h at room temperature and was extracted with diethyl ether (3 × 5.0 mL). The combined organic layers were dried with anhydrous Na_2SO_4 and filtered. Anisole (internal standard) was added, and an aliquot was taken for GC-MS analysis (30 m Rxi-5 ms column, 40−300 °C). Removal of diethyl ether and dissolution in $CDCl_3$ permitted the control also by NMR. Furthermore, the analytical properties of the products are in accordance with commercially available authentic samples.

■ ASSOCIATED CONTENT

Supporting Information

Experimental data such as NMR, APCI-MS, XRD, and calculated WBI and NBO charges. This material is available free of charge via the Internet at http://pubs.acs.org.

■ AUTHOR INFORMATION

Corresponding Author

*E-mail: matthias.driess@tu-berlin.de.

Notes

The authors declare no competing financial interest.

■ ACKNOWLEDGMENTS

Financial support by the Cluster of Excellence UniCat (financed by the Deutsche Forschungsgemeinschaft and administered by the TU Berlin) is gratefully acknowledged. We thank Dr. E. Irran for helping in the XRD structural determinations, Dr. J. Sutter and Prof. Dr. K. Meyer (University of Erlangen) for the ^{57}Fe Mössbauer spectroscopy measurements, and Dr. S. Enthaler (TU Berlin) for fruitful discussions.

■ REFERENCES

(1) (a) Crabtree, R. H. *The Organometallic Chemistry of the Transition Metals*; John Wiley & Sons, Inc.: Hoboken, NJ, 2009. (b) Kamer, P. C. J.; van Leeuwen, P. W. N. M., Eds. *Phosphorus(III) Ligands in Homogeneous Catalysis: Design and Synthesis*; John Wiley & Sons, Ltd.: The Atrium, Southern Gate, Chichester, West Sussex, UK, 2012.

(2) (a) Morales-Morales, D.; Jensen, C. M., Eds. *The Chemistry of Pincer Compounds*; Elsevier: Amsterdam, 2007. (b) van Koten, G.; Milstein, D. *Organometallic Pincer Chemistry*; Springer: Berlin, 2013. (c) Szabo, K. J.; Wendt, O. F., Eds. *Pincer and Pincer-Type Complexes: Applications in Organic Synthesis and Catalysis*; Wiley-VCH Verlag & Co. KGaA: Weinheim, Germany, 2014.

(3) Bart, S. C.; Lobkovsky, E.; Chirik, P. J. *J. Am. Chem. Soc.* **2004**, *126*, 13794−13807.

(4) Bart, S. C.; Chłopek, K.; Bill, E.; Bouwkamp, M. W.; Lobkovsky, E.; Neese, F.; Wieghardt, K.; Chirik, P. J. *J. Am. Chem. Soc.* **2006**, *128*, 13901−13912.

(5) Knijnenburg, Q.; Gambarotta, S.; Budzelaar, P. H. M. *Dalton Trans.* **2006**, 5442−5448.

(6) Danopoulos, A. A.; Wright, J. A.; Motherwell, W. B. *Chem. Commun.* **2005**, 784−786.

(7) Peng, D.; Zhang, Y.; Du, X.; Zhang, L.; Leng, X.; Walter, M. D.; Huang, Z. *J. Am. Chem. Soc.* **2013**, *135*, 19154−19166.

(8) Lagaditis, P. O.; Sues, P. E.; Sonnenberg, J. F.; Wan, K. Y.; Lough, A. J.; Morris, R. H. *J. Am. Chem. Soc.* **2014**, *136*, 1367−1380.

(9) Zell, T.; Milko, P.; Fillman, K. L.; Diskin-Posner, Y.; Bendikov, T.; Iron, M. A.; Leitus, G.; Ben-David, Y.; Neidig, M. L.; Milstein, D. *Chem.—Eur. J.* **2014**, *20*, 4403−4413.

(10) Fürstner, A.; Martin, R.; Majima, K. *J. Am. Chem. Soc.* **2005**, *127*, 12236−12237.

(11) Ung, G.; Rittle, J.; Soleilhavoup, M.; Bertrand, G.; Peters, J. C. *Angew. Chem., Int. Ed.* **2014**, *53*, 8427−8431.

(12) Zhang, H.; Ouyang, Z.; Liu, Y.; Zhang, Q.; Wang, L.; Deng, L. *Angew. Chem., Int. Ed.* **2014**, *53*, 8432−8436.

(13) Langer, R.; Leitus, G.; Ben-David, Y.; Milstein, D. *Angew. Chem., Int. Ed.* **2011**, *50*, 2120−2124.

(14) Yu, R. P.; Darmon, J. M.; Hoyt, J. M.; Margulieux, G. W.; Turner, Z. R.; Chirik, P. J. *ACS Catal.* **2012**, *2*, 1760−1764.

(15) Tondreau, A. M.; Atienza, C. C. H.; Weller, K. J.; Nye, S. A.; Lewis, K. M.; Delis, J. G. P.; Chirik, P. J. *Science* **2012**, *335*, 567−570.

(16) Obligacion, J. V.; Chirik, P. J. *Org. Lett.* **2013**, *15*, 2680−2683.

(17) Blom, B.; Enthaler, S.; Inoue, S.; Irran, E.; Driess, M. *J. Am. Chem. Soc.* **2013**, *135*, 6703−6713.

(18) Brück, A.; Gallego, D.; Wang, W.; Irran, E.; Driess, M.; Hartwig, J. F. *Angew. Chem., Int. Ed.* **2012**, *51*, 11478−11482.

(19) Gallego, D.; Brück, A.; Irran, E.; Meier, F.; Kaupp, M.; Driess, M.; Hartwig, J. F. *J. Am. Chem. Soc.* **2013**, *135*, 15617−15626.

(20) Cope, A. C.; Ciganek, E. *Org. Synth.* **1959**, *39*, 19−22.

(21) Wilson, C. V.; Stenberg, J. F. *Org. Synth.* **1956**, *36*, 48−49.

(22) Park, C. H.; Simmons, H. E. *Org. Synth.* **1974**, *54*, 88−92.

(23) (a) Nakajima, Y.; Nakao, Y.; Sakaki, S.; Tamada, Y.; Ono, T.; Ozawa, F. *J. Am. Chem. Soc.* **2010**, *132*, 9934−9936. (b) Zhang, J.; Gandelman, M.; Herrman, D.; Leitus, G.; Shimon, L. J.; Ben-David, Y.; Milstein, D. *Inorg. Chim. Acta* **2006**, *359*, 1955−1960. (c) O'Reilly, R. K.; Gibson, V. C.; White, A. J.; Williams, D. J. *Polyhedron* **2004**, *23*, 2921−2928. (d) Danopoulos, A. A.; Tsoureas, N.; Wright, J. A.; Light, M. E. *Organometallics* **2004**, *23*, 166−168. (e) Small, B. L.; Brookhart, M.; Bennett, A. M. A. *J. Am. Chem. Soc.* **1998**, *120*, 4049−4050.

(24) Zlatogorsky, S.; Muryn, C. A.; Tuna, F.; Evans, D. J.; Ingleson, M. J. *Organometallics* **2011**, *30*, 4974−4982.
(25) Meyer, S.; Orben, C. M.; Demeshko, S.; Dechert, S.; Meyer, F. *Organometallics* **2011**, *30*, 6692−6702.
(26) Blom, B.; Tan, G.; Enthaler, S.; Inoue, S.; Epping, J. D.; Driess, M. *J. Am. Chem. Soc.* **2013**, *135*, 18108−18120.
(27) Barclay, J. E.; Leigh, G. J. *J. Chem. Soc., Dalton Trans.* **1988**, 2865−2870.
(28) Hawrelak, E. J.; Bernskoetter, W. H.; Lobkovsky, E.; Yee, G. T.; Bill, E.; Chirik, P. J. *Inorg. Chem.* **2005**, *44*, 3103−3111.
(29) Pregosin, P. S. *NMR in Organometallic Chemistry*; Wiley-VCH Verlag & Co. KGaA: Weinheim, Germany, 2012.
(30) Addison, A. W.; Rao, T. N.; Reedijk, J.; van Rijn, J.; Verschoor, G. C. *J. Chem. Soc., Dalton Trans.* **1984**, 1349−1356.
(31) (a) Casey, C. P.; Whiteker, G. T.; Campana, C. F.; Powell, D. R. *Inorg. Chem.* **1990**, *29*, 3376−3381. (b) Pelczar, E. M.; Emge, T. J.; Krogh-Jespersen, K.; Goldman, A. S. *Organometallics* **2008**, *27*, 5759−5767.
(32) Schmedake, T. A.; Haaf, M.; Paradise, B. J.; Millevolte, A. J.; Powell, D. R.; West, R. *J. Organomet. Chem.* **2001**, *636*, 17−25.
(33) Yang, W.; Fu, H.; Wang, H.; Chen, M.; Ding, Y.; Roesky, H. W.; Jana, A. *Inorg. Chem.* **2009**, *48*, 5058−5060.
(34) Tobita, H.; Matsuda, A.; Hashimoto, H.; Ueno, K.; Ogino, H. *Angew. Chem., Int. Ed.* **2004**, *43*, 221−224.
(35) Bart, S. C.; Lobkovsky, E.; Bill, E.; Wieghardt, K.; Chirik, P. J. *Inorg. Chem.* **2007**, *46*, 7055−7063.
(36) Blom, B. *Reactivity of Ylenes at Late Transition Metal Centers*; Doctoral Thesis, Rheinische Friedrich-Wilhelms-University of Bonn, April 2011.
(37) Darmon, J. M.; Yu, R. P.; Semproni, S. P.; Turner, Z. R.; Stieber, C. E.; DeBeer, S.; Chirik, P. J. *Organometallics* **2014**, *33*, 5423−5433.
(38) (a) Wiberg, K. B. *Tetrahedron* **1968**, *24*, 1083−1096. (b) Irwin, R. P. *Organometallic Chemistry: Research Perspectives*, 1st ed.; Nova Science Pub Inc.: Hauppauge, NY, 2008; p 292.
(39) Trovitch, R. J.; Lobkovsky, E.; Chirik, P. J. *Inorg. Chem.* **2006**, *45*, 7252−7260.
(40) (a) Enthaler, S.; Junge, K.; Beller, M. *Angew. Chem., Int. Ed.* **2008**, *47*, 3317−3321. (b) Morris, R. H. *Chem. Soc. Rev.* **2009**, *38*, 2282−2291. (c) Zhang, M.; Zhang, A. *Appl. Organomet. Chem.* **2010**, *24*, 751−757.
(41) Sen, S. S.; Roesky, H. W.; Stern, D.; Henn, J.; Stalke, D. *J. Am. Chem. Soc.* **2010**, *132*, 1123−1126.
(42) Nagendran, S.; Sen, S. S.; Roesky, H. W.; Koley, D.; Grubmüller, H.; Pal, A.; Herbst-Irmer, R. *Organometallics* **2008**, *27*, 5459−5463.
(43) Karsch, H. H.; Klein, H.-F.; Schmidbaur, H. *Angew. Chem., Int. Ed.* **1975**, *14*, 637−638.
(44) Sheldrick, G. M. *SHELX-97: Program for Crystal Structure Refinement*; University of Göttingen: Göttingen, Germany, 1997.